의학박사 학위논문

골수 중배엽 줄기 세포의 노화가 BMP-2에 의한 줄기 세포 분화에 미치는 영향

Senescence dependent BMP-2 effect on bone marrow mesenchymal stem cell differentiation

2018년 2월

서울대학교 대학원
의학과 정형외과학 전공
조 재 환

골수 중배엽 줄기 세포의 노화가 BMP-2에 의한 줄기 세포 분화에 미치는 영향

지도교수 이 춘 기

이 논문을 의학과 박사 학위논문으로 제출함

2018년 1월

서울대학교 대학원

의학과 정형외과학 전공

조 재 환

조재환의 의학박사 학위논문을 인준함

2018년 1월

위원장	김 인 규	(인)
부위원장	이 춘 기	(인)
위원	이 재 협	(인)
위원	김 희 찬	(인)
위원	이 동 호	(인)

Senescence dependent BMP-2 effect on bone marrow mesenchymal stem cell differentiation

by

Jae Hwan Cho

A Thesis Submitted in Partial Fulfillment of the
Requirements for the Degree of Doctor of Philosophy
in Medicine (Orthopedics)
at the Seoul National University, College of Medicine

January 2018

Approved by thesis committee:

Professor In-Gyu Kim Chairman

Professor Choon-Ki Lee Vice chairman

Professor Jae Hyup Lee

Professor Hee Chan Kim

Professor Dong-Ho Lee

Abstract

Background: Mesenchymal stem cells (MSCs) are cells having potential to differentiate various type of cells including osteoblasts, adipocytes, or chondrocytes. Bone morphogenetic protein-2 (BMP-2) is considered as a powerful inducer to promote cascade of differentiation into osteoblasts. Recently, BMP-2 has been tried as a bone graft substitute when spinal fusion surgery is performed in old age patients. However, lack of knowledge about the differentiation of MSCs by BMP-2 and the effect of aging has been one of problems for extensive use of BMP-2. In this regard, we intended to compare the effect of recombinant human BMP-2 (rhBMP-2) on differentiation of MSCs into osteoblasts and adipocytes between aging MSCs and young (control) MSCs.

Materials and methods: Cellular aging (senescence) was induced by replicative passages with cultures under high level glucose. Senescence-associated ß-galactosidase (SA-ß-gal) staining, and senescence related markers (p16, p21, and p53) were used to confirm aging MSCs. Aging and young (control) MSCs were cultured in osteogenic and adipogenic differentiated medium with different concentration of BMP-2 (0, 25, 100, 250, and 500 ng/ml). We compared the phenotypes by Calcium assay, adipogenesis assay, and specific staining (Alkaline Phosphatase, Alizarin Red S, Oil red O), and gene expression patterns by real-time polymerase chain reaction (PCR),

western blot assay, and microarray analyses between aging MSCs and control MSCs. Microarray analysis was conducted with 4 different cells (aging MSCs and control MSCs with or without the induction of BMP-2). GSEA (Gene Set Enrichment Analysis), leading-edge subset analysis, and MetaCore analysis were used as a microarray analysis.

Results: Aging cells by replicative passages under high level glucose (22 mM) were well characterized by senescence markers. Osteogenic differentiation by BMP-2 decreased in aging MSCs compared to control MSCs. Lower ALP activity and less Ca^{++} release was observed in aging MSCs ($P < 0.001$, and $P = 0.005$, respectively), and positive dose-response relationship was observed in both MSCs. The mRNA expression of Runx-2, bone sialoprotein (BSP) and osteocalcin (OCN) was lower in aging MSCs. However, adipogenic differentiation by BMP-2 was comparable between 2 cells. Adipogenesis assay showed no differences of adipogenic potential between 2 groups ($P = 0.279$). In addition, there was no superiority in the expression of PPARγ between 2 cells. These results were also supported in protein level by western blot assay.

Microarray analysis showed more upregulated genes in rhBMP-2-treated aging MSCs than in rhBMP-2-treated control MSCs and non-treated aging MSCs. Aging and adipogenesis related gene sets were more upregulated and significantly enriched by the induction of rhBMP-2 in aging MSCs compared to control MSCs. In BMP related leading edge subsets, 6 clustered genes (CHRDL1, NOG, SMAD1, SMAD7, FST, and BAMBI) were upregulated in

aging MSCs. In aging MSCs, NF-kB or p38 MAPK pathway could be important in response to BMP-2, whereas BMP/SMAD pathway in young MSCs, based on MetaCore analysis.

Conclusions: Aging MSCs showed less osteogenic differentiation and comparable adipogenic differentiation in response to BMP-2 compared to control MSCs. Relative superior adipogenic differentiation by BMP-2 in aging MSCs is supported by the result of microarray analysis. In addition, several genes might be candidates for senescence dependent BMP-2 effect on differentiation of MSCs. Different signaling pathway might play a role in different response to BMP-2 between aging and young MSCs. Further in vivo research along with the current study may contribute to effective use of BMP-2 in clinical fields by elucidating the signaling pathway whether MSCs differentiate into osteoblasts or adipocytes by BMP-2.

Keywords: mesenchymal stem cell; bone morphogenetic protein; BMP-2; differentiation; aging; senescence; osteoblast; adipocyte; microarray

Student Number: 2012-31133

Table of Contents

List of Tables

List of Figures

Introduction

Mesenchymal stem cells (MSCs) are cells having potential to differentiate various type of cells including osteoblasts, adipocytes, or chondrocytes (Chamberlain et al. 2007). MSCs were originally identified in the bone marrow. Because the number of MSCs in the bone marrow is relatively scarce, human adipose-derived MSCs (ASCs) or umbilical cord MSCs (UMSCs) have been used as alternatives to reveal the characteristics of MSCs. However, the role of these alternative MSCs for the formation of bone has not been clearly defined. For example, it was reported that ectopic bone formation by ASCs is less sufficient than that by bone marrow derived MSCs (BMSCs) (Im et al. 2005, Vishnubalaji et al. 2012). In addition, UMSCs showed an absent trilineage differentiation capacity in vitro (Bosch et al. 2012). So, BMSCs have been considered as ideal subject to reveal the differentiation potential into osteoblasts or adipocytes regardless of its scarcity.

The differentiation potential of MSCs was decided by specific stimuli or environments (Gregory et al. 2005, Pino et al. 2012, Rippo et al. 2013, Fotia et al. 2015). Several stimulating factors to induce differentiation of MSCs into various phenotypes have been researched so far (Dingwall et al. 2011, Yu et al. 2012, Matsumoto et al. 2013, Byun et al. 2014, Berendsen et al. 2015). Interestingly, an inverse correlation between osteogenesis and adipogenesis

has been suggested (Pei et al. 2004). For example, peroxisome proliferator-activated receptor-γ (PPAR-γ) deficient mice showed higher bone formation with failure to differentiate into adipocytes (Akune et al. 2004). It was proposed that disruption of BMP signaling by BMP receptor 1A conditional knockout mice increased endogenous bone formation with reduced osteoclastogenesis (Kamiya et al. 2008). In general, it is known that BMP receptor 1A induces adipogenic effect.

Wnt signaling, Hedgehog signaling, NELL-1 (NEL-like protein 1) signaling, and insulin-like growth factor (IGF) signaling were suggested as one of determinant signaling pathways for differentiation into osteoblasts or adipocytes (Fontaine et al. 2008, Plaisant et al. 2009, Crane et al. 2013, Shen et al. 2016, Xu et al. 2016). However, complex cross-talk among various pathways and transcription factors make it hard to draw a conclusion about the differentiation of MSCs.

Among them, bone morphogenetic protein-2 (BMP-2) is considered as a powerful inducer to promote cascade of differentiation into osteoblasts (Wang et al. 1993). The mechanism of the differentiation has not been fully understood. It was proposed that differentiation into osteoblast lineage was initiated by stimulation of BMP-2 receptor IB, followed by phosphorylation of R-Smad (Smad 1/5/8), and activation of several transcription factors such as Runt-related transcription factor 2 (Runx2) or osterix (Wang et al. 1993, Kato et al. 2009). Whereas, it was proposed that BMP-2 receptor IA,

CCAAT/enhancer-binding protein (C/EBP), and peroxisome proliferator-activated receptor-γ (PPAR-γ) are key regulators to differentiation into the adipocyte lineage (Wu et al. 2010, Scott et al. 2011). In this process, it was known that complex signaling pathways exist and have cross-talk one another (Zhang et al. 2011, Zhuang et al. 2016). For example, PPAR-γ also have a role in osteoblastogenesis as well as adipogenesis (Zhang et al. 2015, Yuan et al. 2016). However, clear mechanism about the signaling pathway to decide the fate of MSCs has not been determined.

In this background, BMP-2 has also been researched as a bone graft substitute in the clinical area of orthopedic or dental surgery (Coomes et al. 2014, Cho et al. 2017). However, its clinical applications are limited by the lack of an effective carrier, complications, and high cost. Furthermore, the lack of knowledge in differentiation of MSCs is critical to disturb its clinical use. In some conditions, MSCs mainly differentiate into adipocytes instead of osteoblasts by the application of BMP-2, which can be troublesome. For example, MSCs from osteoporotic patients showed no response to exogenous BMP-2, which means the failure of differentiation into osteoblast by BMP-2 under adipogenic conditions (Donoso et al. 2015).

Spinal fusion by instrumentation and bone graft has been the mainstay of spinal surgery. The incidence of spinal fusion and the mean age of patients has been recently increasing because quality of life is a serious consideration and surgical technique has been rapidly developed (Bae et al. 2013). In this

background, BMP-2 has been also tried to enhance fusion rate in spinal surgery, however, its mechanism of action is unclear (Singh et al. 2014). Furthermore, the effect of BMP-2 into MSCs in old populations might be different with that in young populations. Thus, the research about the differentiation of aging MSCs by BMP-2 can be meaningful to apply to its clinical use.

In this regard, the main purpose of this study is to compare the effect of recombinant human BMP-2 (rhBMP-2) on differentiation of BMSCs into osteoblasts and adipocytes between aging MSCs and young (control) MSCs. Past in vitro and in vivo studies showed controversial results about the effect of aging on the osteoinductive activity of rhBMP-2. It was reported that bone formation by rhBMP-2 decreased in aging rats (Hara et al. 2015). However, it was proposed that decreased adipogenic and increased osteogenic lineage was induced by replicative senescence (Cheng et al. 2010). In other study, both osteogenesis and adipogenesis decreased as the number of passage increased. However, differentiation into adipocytes decreased more markedly than that into osteocytes (Bonab et al. 2006). However, above-mentioned in vitro studies about the effect of replicative senescence on the differentiation of MSCs did not evaluate the effect of rhBMP-2. In order to reveal the dose-dependent effect of BMP-2 on the differentiation of BMSCs into osteoblasts or adipocytes according to cellular senescence, various concentrations of rhBMP-2 were used in the current study. Microarray analysis was performed

to compare gene expression between aging and control MSCs treated with or without rhBMP-2.

Microarray analysis is used to interpret the data including a large number of genes from samples of DNA, RNA, or protein. The concept of this technique was developed in 1983, and specific 'gene chip' technique was introduced by using a complementary DNA in 1995 (Chang 1983, Schena et al. 1995). Microarray analysis involves several steps such as background correction, quality control, spot filtering, aggregation and normalization, identification of significant differential expression, and pattern recognition. For evaluation of relative gene expression, gene set enrichment analysis (GSEA) with leading edge subset analysis, and MetaCore analysis were used. With these specific technique, differences of gene expression pattern and relevant signaling pathway between aging and control MSCs could be evaluated.

Materials and methods

Cellular aging (senescence) was induced by replicative passages with cultures under high level glucose until further differentiation barely progressed (Cheng et al. 2010, Chang et al. 2015). Senescence-associated ß-galactosidase (SA-ß-gal) staining and expression of senescence markers (p16, p21, and p53) confirmed that MSCs at P7 were senescent. Aging and control MSCs were cultured in osteogenic and adipogenic differentiation medium containing various concentrations of rhBMP-2 (0, 25, 100, 250, and 500 ng/ml). The phenotypes and gene expression patterns of these cells were compared by performing staining, real-time polymerase chain reaction (PCR), western blotting, and microarray analysis.

Preparation of aging MSCs and control MSCs

Commercial human BM-derived MSCs were obtained from Lonza (Walkersville, USA). To obtain aging MSCs, cells were cultured for 3 days and then split at a ratio of 1:3. After four passages, cells were incubated in culture medium containing 22 mM glucose for a further three passages. Cells cultured for four passages were used as control MSCs. MSCs were routinely cultured in mesenchymal stem cell growth medium (MSCGM™) (Lonza) at 37.9°C in 5% CO_2.

Markers for cellular senescence

Both MSCs were plated in six-well plate. Senescence-associated ß-galactosidase (SA-ß-gal) staining was performed by the manufacture's instruction (Cell Signaling Technology, Inc, USA). Cells were observed under inverted microscope. The proportion of SA-ß-gal positive cells as well as the intensity of staining were considered as senescence markers. In addition, the higher protein expression of p16, p21, and p53 was considered as molecular markers for cellular senescence.

Preparation of bone morphogenetic protein-2 (BMP-2)

E.coli-derived recombinant human BMP-2 (Novosis, Bioalpha Inc., Gyeonggi-do, Korea) was used for this study. The stock solution was prepared with Dulbecco's PBS to obtain 25, 100, 250, and 500 µg/ml rhBMP-2. Then, the solution was mixed into the differentiation medium to obtain 25, 100, 250, and 500 ng/ml of rhBMP-2.

Osteogenic differentiation

Differentiation of aging and control MSCs into osteoblasts was performed in osteoblastic differentiation media containing MSCGM supplemented with 10% FBS, 1% antibiotics, 10 nM dexamethasone, 10 mM ß-glycerophosphate, and 100 µM L-ascorbic acid-2-phosphate (Sigma-Aldrich.Inc., USA). The media were changed every 3 days, and cells were cultured for about 14 days.

Adipogenic differentiation

Differentiation of aging and control MSCs into adipocytes was performed in adipocyte differentiation media containing MSCGM supplemented with 10% FBS, 1% antibiotics, 0.5 mM 1-methyl-3-isobutylxanthine (Sigma-Aldrich.Inc.), 1 μM dexamethasone (Sigma-Aldrich.Inc.), 10 μM insulin (Sigma-Aldrich.Inc.), and 100 μM indomethacin (Sigma-Aldrich.Inc.). The media were changed every 3 days, and cells were cultured for about 14 days.

RNA isolation and real time PCR

Total RNA was isolated by using Qiagen RNA isolation kit according to manufacturer's instruction. Total RNA 1 μg was reverse-transcribed by using cDNA reverse transcription kit (Intron Biotechnology, Inc., Korea). GAPDH was used to normalize the level of gene expression. Real-time PCR was conducted by system using LightCycler® 480 (Roche Molecular Systems, Inc. Basel, Switzerland). Primer sequences of each genes for PCR were summarized in Table 1.

Table 1. Primer sequences of genes for real time PCR

Gene	Primer Forward	Primer Reverse
p16	GGG GGC ACC AGA GGC AGT	GGT TGT GGC GGG GGC AGT T
p21	GAG GCC GGG ATG AGT TGG GAG GAG	CAG CCG GCG TTT GGA GTG GTA GAA
p53	CCC CTC CTG GCC CCT GTC ATC TTC	GCA GCG CCT CAC AAC CTC CGT CAT
ALP	ACC ATT CCC ACG TCT TCA CAT TT	AGACATTCTCTCGTTCAC CGCC
RUNX2	ATT TCT CAC CTC CTC AGC CC	CAA CAG CCA CAA GTT AGC GA
BSP	CGA ATA CAC GGG CGT CAA TG	GTA GCT GTA CTC ATC TTC ATA GGC
OCN	GGC GCT ACC TGT ATC AAT GG	TCAGCCAACTCGTCACA GTC
GAPDH	CGA GAT CCC TCC AAA ATC AA	TTCACACCCATGACGAA CAT

ALP: alkaline phosphatase; RUNX2: Runt-related transcription factor 2; BSP: bone sialoprotein; OCN: osteocalcin; GAPDH: glyceraldehyde 3-phosphate dehydrogenase

Western blot assays

After washing the cells using cold PBS buffer, total protein was isolated with lysis buffer supplemented with protease inhibitor cocktail (Sigma-Aldrich. Inc.) and quantified using BCA protein assay kit (Pierce, USA). Proteins separated on 12% of SDS-PAGE and transferred to the PVDF membrane. Blotted membrane was 5% skim milk blocked for 1 h at room temperature and probed with corresponding antibodies (p21, p16, p53, ALP, RUNX2, BSP, OCN, PPARγ, beta-actin) overnight at 4℃. After incubation with peroxidase-conjugated secondary antibody (Cell Signaling Technology, Inc.) for 1 h at room temperature, membrane was incubated with ECL western blotting substrate (Thermo Fisher Scientific Inc., USA) for 1 min at room temperature. Digital imaging is usually performed with the ImageQuant LAS 4000 (GE Healthcare Bio-Sciences Corp., USA) and qualitative protein analysis is performed in order to verify the presence or absence of a specific protein.

Alkaline phosphatase (ALP) staining, activity, and quantification

ALP staining and activity was performed after 3, 7, and 14 days of osteoblastic induction. For ALP activity assay, cells were lysed with 0.2% TX-100 solution at 37℃ incubator for 30 min. ALP activity was determined by incubation with P-nitrophenyl phosphate (pNPP) (Sigma-Aldrich.Inc) and lysed sample at 37°C for 20 min, p-nitrophenol was used as a standard to determine enzyme activity. The activity was stopped by addition of 3 M NaOH, and reaction absorbance was measured at 405 nm by using microplate

reader (SpectraMax Plus 384 Microplate Reader, Molecular Devices, LLC., USA). For ALP staining, cells were washed 2 times with PBS and incubated for 10 min with ALP substrate staining solution containing 0.01% Naphtol-AS-MX-phosphate solution (Sigma-Aldrich.Inc) and Fast blue RR salt (Sigma-Aldrich.Inc) dissolved in H_2O.

Calcium assay

Both MSCs were plated at 24-well plates containing osteoblastic differentiated medium in various conditions described for 14 days. Calcium assay kit (BioAssay system, CA, USA) was used to measure calcium determination. Cells were treated with 100 μl of 0.5% HCl, and incubated at room temperature for 5 min. Then the suspension was collected to the new tube, and standard curve was generated by using calcium in calcium assay kit according to manufacturer's instruction. Each sample was transferred into 96-well plates, and treated with 200 μl of working reagent in the kit, and incubated at room temperature for 3 min. Absorbance of samples was read at 612 nm by using microplate reader (SpectraMax Plus 384 Microplate Reader, Molecular Devices, LLC., USA).

Alizarin red S (ARS) staining

AR-S staining was performed after 14 days of osteoblastic induction. Cells were washed with PBS, then added AR-S (Sigma-Aldrich.Inc) dissolved in distilled water. The cells were stained for 10 min at room temperature. The degree of calcium deposition was visualized under the microscope.

Oil red O (ORO) staining

ORO staining was performed after 14 days of adipogenic induction. Cells were washed with PBS and fixed using the provided fixative solution at room temperature for 15 min. After removing the fixative, cells were washed with diH2O and stained with Oil Red O (ScienCell Research Laboratories, Inc.) for 15 min at room temperature. The samples were visualized under the microscope.

Adipogenesis assay

Adipogenesis assay kit (Abcam, UK) was used to measure lipid formation after 14 days of MSC differentiation under adipogenic medium. Cells were washed with Dulbecco's PBS. Then dye extraction solution (provided by the manufacture of the assay kit) was added, and sealed plates were incubated at 90-100℃ for 30 min, followed by cooling. Lipase was added to each sample and standard, and incubated for 10 min. Then, reaction mix solution in the kit was treated and incubated at room temperature for 30 min. Absorbance of samples was read at 535/587 nm by using microplate reader.

Statistical Analysis

All experiments were conducted for 3 times and taking the average values. Independent t-test or ANOVA (analysis of variance) was used. Statistical analyses were performed using the Statistical Package for Social Sciences

software package (version 21.0, SPSS, Chicago, IL). *P* values less than 0.05 were considered statistically significant.

Microarray analysis

To compare gene expression according to the concentration of BMP-2 and aging of MSCs, microarray analysis was conducted for 4 types of RNA samples (aging MSCs without induction of BMP-2, control MSCs without induction of BMP-2, aging MSCs cultured in BMP-2 (250 ng/ml for 3 days), and control MSCs cultured in BMP-2 (250 ng/ml for 3 days). Three identical RNA samples in each type (total 12 samples) were used to analyze.

RNA quality check

RNA purity and integrity were evaluated by ND-1000 Spectrophotometer (NanoDrop, Wilmington, USA), Agilent 2100 Bioanalyzer (Agilent Technologies, Palo Alto, USA).

Affymetrix whole transcript expression arrays methods

The Affymetrix Whole transcript Expression array process was executed according to the manufacturer's protocol (GeneChip Whole Transcript PLUS reagent Kit). The cDNA was synthesized using the GeneChip WT (Whole Transcript) Amplification kit as described by the manufacturer. The sense cDNA was then fragmented and biotin-labeled with TdT (terminal deoxynucleotidyl transferase) using the GeneChip WT Terminal labeling kit.

Approximately 5.5 μg of labeled DNA target was hybridized to the Affymetrix

GeneChip Human 2.0 ST Array at 45°C for 16 h. Hybridized arrays were washed and stained on a GeneChip Fluidics Station 450 and scanned on a GCS3000 Scanner (Affymetrix).

Signal values were computed using the Affymetrix® GeneChip™ Command Console software.

Raw data preparation and Statistic analysis

Raw data were extracted automatically in Affymetrix data extraction protocol using the software provided by Affymetrix GeneChip® Command Console® Software (AGCC). After importing CEL files, the data were summarized and normalized with robust multi-average (RMA) method implemented in Affymetrix® Expression Console™ Software (EC). We exported the result with gene level RMA analysis and performed the differentially expressed gene (DEG) analysis.

Statistical significance of the expression data was determined using independent t-test and fold change in which the null hypothesis was that no difference exists among groups. False discovery rate (FDR) was controlled by adjusting *P* value using Benjamini-Hochberg algorithm (Sabatti et al. 2003). For a DEG set, hierarchical cluster analysis was performed using complete linkage and Euclidean distance as a measure of similarity.

Gene-Enrichment and Functional Annotation analysis for significant probe list was performed using Gene Ontology (www.geneontology.org/) and KEGG(www.genome.jp/kegg/). All data analysis and visualization of differentially expressed genes was conducted using R 3.1.2 (www.r-

project.org)

Gene expression profile analysis

1. Gene Set Enrichment Analysis (GSEA)

Functional analysis of the 20-cell microarray database was performed using GSEA and leading-edge subset analysis (Broad Institute, Cambridge, MA, USA). For general global transcriptome comparison, GSEA based on a curated functional gene sets (C2) database was set with a permutation number of '1000', 'collapse dataset to gene symbols' as 'true' and permutation type as 'phenotype'. The C2 functional gene set collections were based on online pathway databases, publications in PubMed and knowledge of the domain. By default, gene sets were ordered by a normalized enrichment score (NES).

The GSEA results were suggested by enrichment plots and heat maps with enrichment score (ES), NES, FDR, and nominal *P* value. ES is calculated by walking down the ranked list of genes, increasing a running-sum statistic when a gene is in the gene set and decreasing it when it is not. NES is the value of actual ES divided by mean (ESs against all permutations of the dataset), which can be used to compare results across gene sets. The FDR is the estimated probability that a gene set with a given NES represents a false positive finding.

Significant enrichment of gene sets was determined by both FDR < 25% and nominal $P < 0.05$ in this study.

In a heat map, expression values are represented as colors, where the range of colors (red, pink, light blue, dark blue) shows the range of expression values (high, moderate, low, lowest).

2. MetaCore analysis

MetaCore is an integrated software suite for functional analysis of experimental data. MetaCore is based on a curated database of human protein-protein, protein-DNA interactions, transcription factors, signaling and metabolic pathways, disease and toxicity, and the effects of bioactive molecules. Functional analysis of gene expression profile, pathway analysis, and enrichment analysis was conducted by using MetaCore. The list of significantly expressed genes were filtered by the following cut-off values; fold change > 1.4 and $P < 0.001$.

Results

Comparisons of senescence markers between aging and control MSCs

SA-ß-gal staining of MSCs was illustrated in Fig. 1. More SA-ß-gal (+) cells were observed in aging MSCs (P7) than in control MSCs (P4). The number of SA-ß-gal (+) cells increased with passages.

Fig. 1. SA-ß-gal staining of aging (P7) and control (P4) MSCs

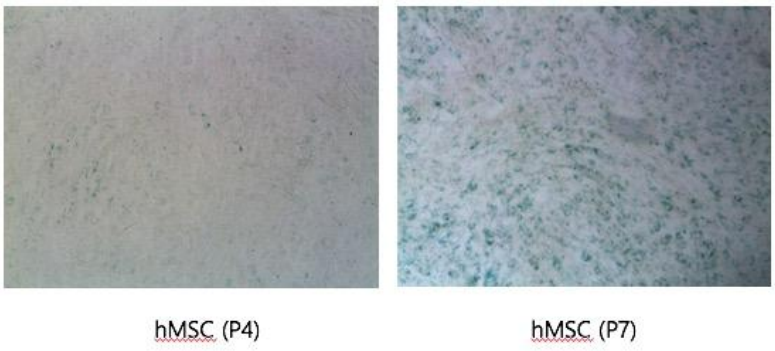

The mRNA expression of p16, p21, and p53 was compared by real-time PCR (Fig. 2a). The expression of p16, p21, and p53 in aging MSCs (P7) was higher in aging MSCs (P7) than in control MSCs (P4) ($P < 0.01$, respectively). Protein expression of these senescence markers was also higher in aging MSCs than in control MSCs (Fig. 2b). We further investigated with aging MSCs (P7 with glucose) and control MSCs (P4).

Fig. 2a. mRNA expression of p16, p21, and p53 in MSCs by the number of passage and treatment of high glucose.

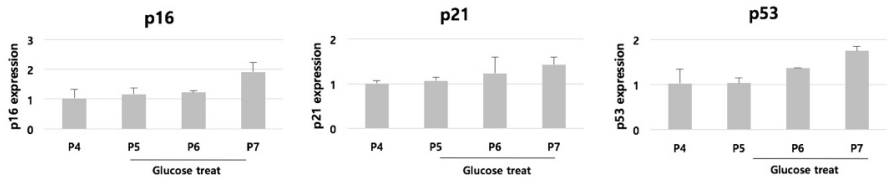

Fig. 2b. Protein expression of p16, p21 and p53 in MSCs by the number of passage and treatment of high glucose. Beta-actin was used as an internal control.

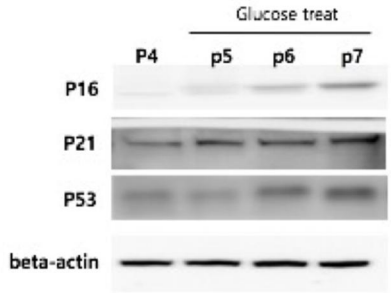

Comparisons of mineralization markers between aging and control MSCs upon osteogenic differentiation in the presence of rhBMP-2

ALP activity and staining

ALP activity after 3 days of culture in osteogenic differentiation showed no difference between aging and control MSCs. However, ALP activity was lower in aging MSCs than in control MSCs after 7 and 14 days of culture containing various concentrations of rhBMP-2 ($P < 0.001$). In addition, ALP activity was higher after 7 days than after 3 days ($P < 0.001$). Although ALP

activity was not higher after 14 days than after 7 days (P = 0.976), rhBMP-2 increased ALP activity in a dose-dependent manner at both of these time points (Fig. 3a). Similar findings were made when examining ALP staining (Fig. 3b). Dose-dependent and time-dependent relationship was found in both cells. However, the degree of ALP staining was lower in aging MSCs than in control MSCs.

Fig. 3a. Alkaline phosphatase (ALP) activity of aging and control MSCs by the induction of BMP-2

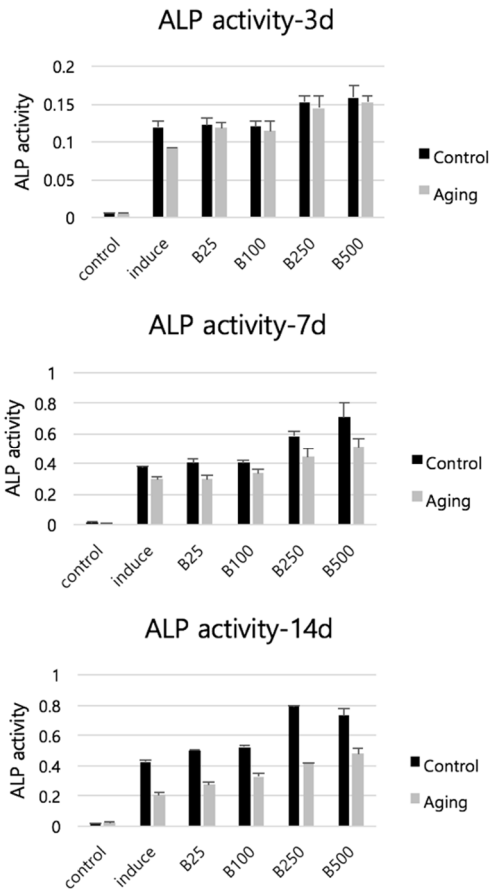

Fig. 3b. Alkaline phosphatase (ALP) staining of aging and control MSCs by the induction of BMP-2

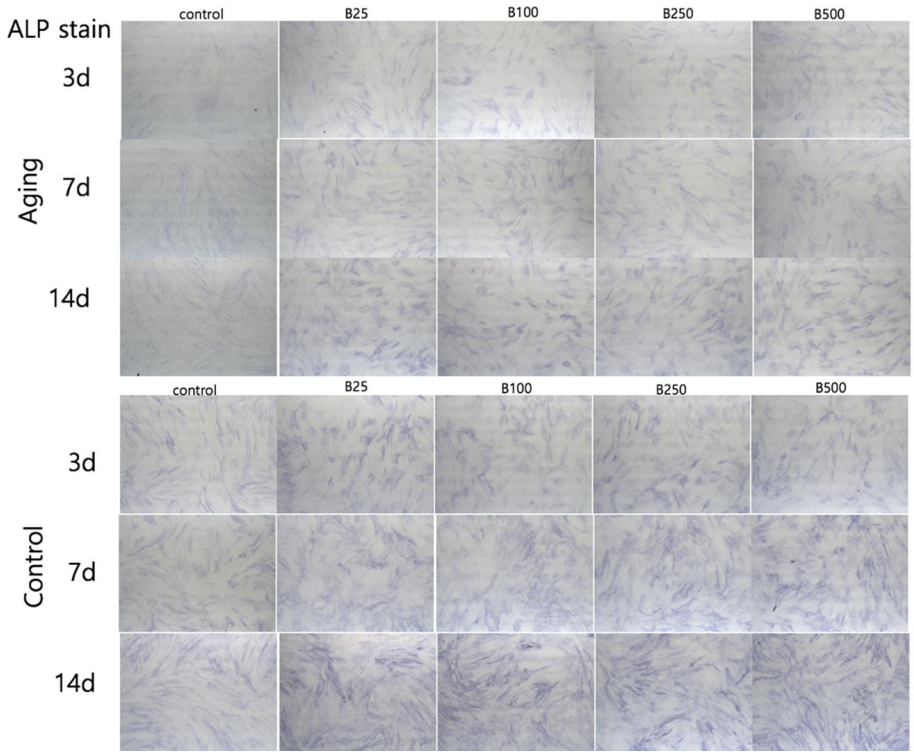

Calcium assay and ARS staining

Aging MSCs released less Ca^{2+} than control MSCs upon osteogenic differentiation, and rhBMP-2 treatment increased Ca^{2+} release in a dose-dependent manner (Fig. 4a, $P = 0.005$). The gap between aging cells and control cells is greater as the concentration of BMP-2 increase. The Ca^{2+} release under 500 ng/ml of BMP-2 decreased by about 40% in aging MSCs compared to control MSCs, whereas the Ca^{2+} release under 25 ng/ml of BMP-2 decreased by about 15%. Moreover, ARS staining was more intense in control MSCs than in aging MSCs upon osteogenic differentiation (Fig. 4b).

Fig. 4a. Calcium assay of aging and control MSCs by the induction of BMP-2

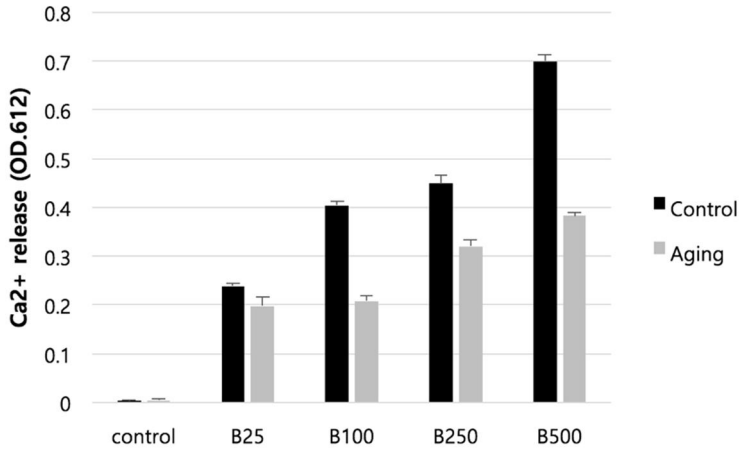

Fig. 4b. Alizarin Red S (ARS) staining of aging and control cells by the induction of BMP-2 (14 days)

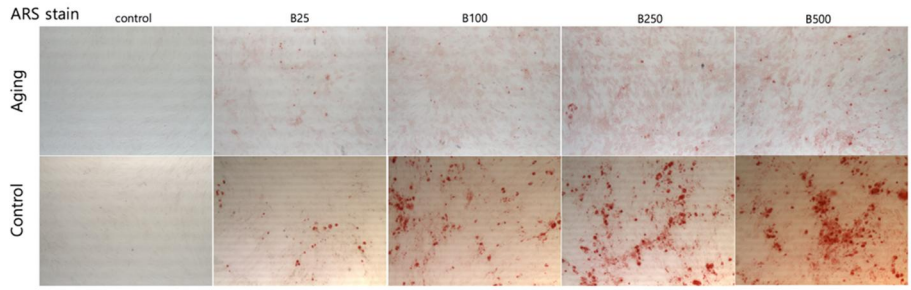

Comparisons of adipogenesis markers between aging and control MSCs upon adipogenic differentiation in the presence of rhBMP-2

Adipogenesis assay and ORO staining

Adipogenic activity was slightly lower in aging MSCs than in control MSCs upon culture in adipogenic differentiation medium containing various concentrations of rhBMP-2; however, this difference was not statistically

significant (P = 0.279). rhBMP-2 increased adipogenic activity in a dose-dependent manner (Fig. 5a). In addition, ORO staining did not markedly differ between aging and control MSCs upon adipogenic differentiation (Fig. 5b)

Fig. 5a. Adipogenesis assay of aging and control MSCs by the induction of BMP-2 (RFU: Relative Fluorescence Units)

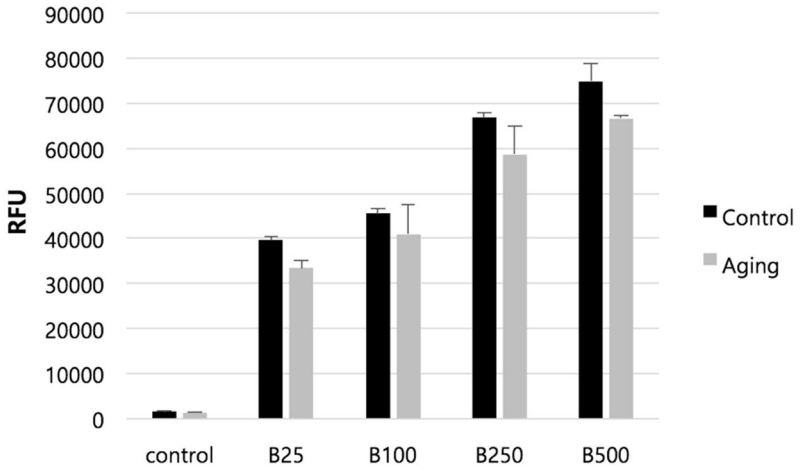

Fig. 5b. Oil Red O staining of aging and control MSCs by the induction of BMP-2

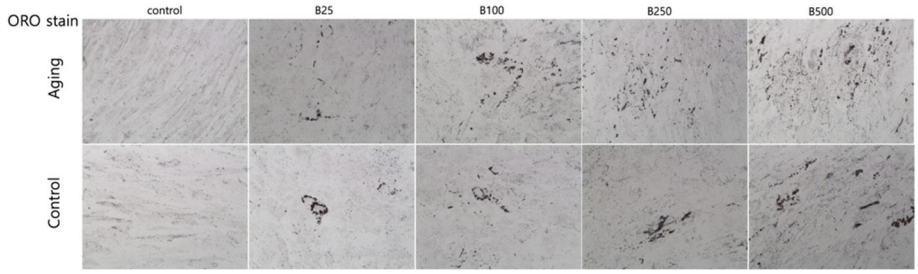

Expression of transcription factors in aging and control MSCs upon differentiation in the presence of rhBMP-2

Real-time PCR

The mRNA expression of ALP, BSP, and OCN was lower in aging MSCs than in control MSCs after 7 and 14 days of culture in osteogenic differentiation medium containing various concentrations of rhBMP-2, but did not differ between the two groups of cells after 3 days (Fig. 6a). rhBMP-2 dose-dependently increased mRNA expression of all three markers in control MSCs after 7 and 14 days. In addition, rhBMP-2 increased mRNA expression of BSP and OCN in control MSCs in a time-dependent manner. By contrast, rhBMP-2 only slightly increased mRNA expression of ALP in a dose-dependent manner in aging MSCs, and did not affect that of BSP or OCN.

The mRNA expression of ALP (alkaline phosphatase), BSP (bone sialoprotein), and OCN (osteocalcin) in aging and control MSCs was shown in Fig. 6a. Although the expression of ALP, BSP, and OCN detected in 3 days are not different between 2 groups, less expression was evident in aging MSCs compared to control MSCs detected in 7 and 14 days under every concentration of BMP-2 induction. In addition, dose-dependent relationship was found in the expression of ALP, BSP, and OCN in control cells detected in 7 and 14 days. In addition, time-dependent relationship was found in the expression of BSP and OCN in control cells. However, no further expression of BSP and OCN was found by the induction of BMP-2 in aging MSCs although a little more expression of ALP by the BMP-2 with dose-dependent manner.

Fig. 6a. The relative expression of ALP, BSP, and OCN in aging and control MSCs (3, 7, 14 days)

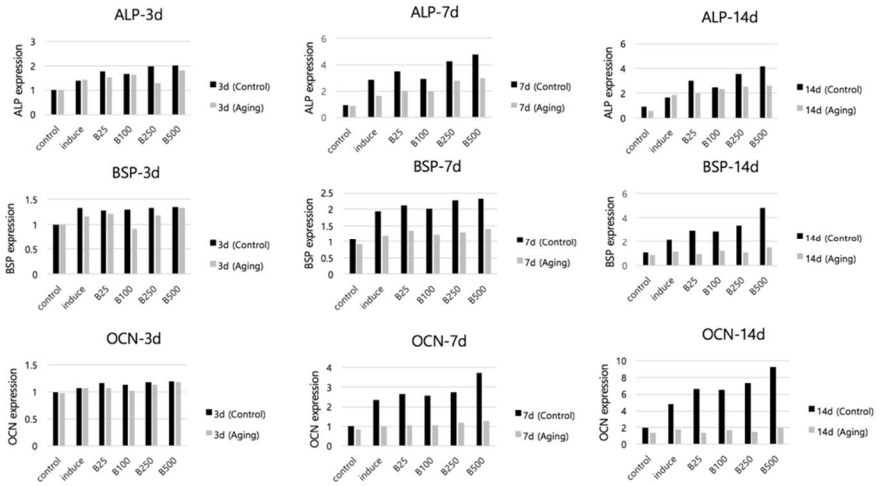

The mRNA expression of Runx2 and PPARγ expression was shown in Fig. 6b. The mRNA expression of Runx2 was lower in aging MSCs than in control MSCs after 3 and 7 days of culture in osteogenic differentiated medium. However, PPARγ expression did not differ between aging and control MSCs and was increased by rhBMP-2 in a dose-dependent manner.

Fig. 6b. The relative expression of Runx2 and PPARγ in aging and control MSCs (3, 7, 14 days)

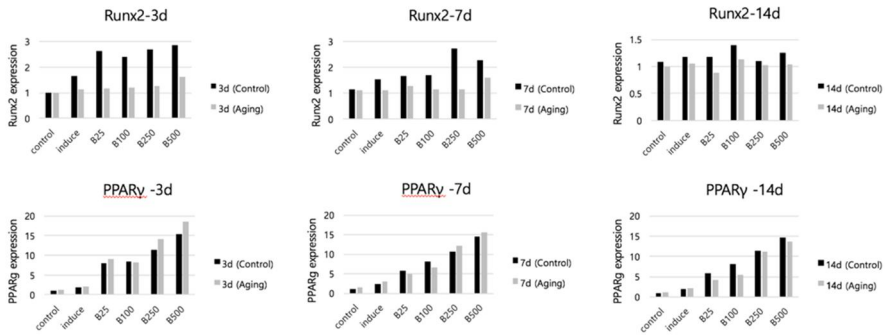

Western blot assay

Western blotting of ALP, Runx2, BSP, OCN, and PPARγ is shown in Figure 7. Expression of these proteins was higher after 7 days than after 3 days of culture. However, protein expression of ALP, Runx2, BSP, and OCN was lower in aging MSCs than in control MSCs. Treatment with 500 ng/ml rhBMP-2 for 7 days slightly increased expression of these four markers in aging MSCs. However, no discernable difference could be found in expression of PPARγ.

Fig. 7. Protein expression of ALP, Runx2, BSP, OCN, and PPARγ in control and aging MSCs under different concentration of BMP-2. Beta-actin was used as an internal control.

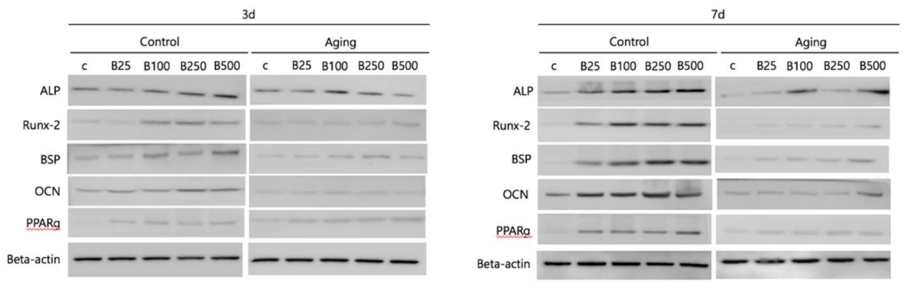

Microarray analysis

Data quality check

Hierarchical clustering and multidimensional scaling revealed well-qualified samples with each type specificity, which means the good quality of provided samples (Fig. 8). Each sample was designated as follows: phenotype A (N_1,

N_2, N_3): RNA from aging MSC without induction of BMP-2; phenotype B (N_4, N_5, N_6): RNA from aging MSC with induction of BMP-2 (250 ng/ml, 3 days); phenotype C (N_7, N_8, N_9): RNA from control MSC without induction of BMP-2; phenotype D (N_10, N_11, N_12): RNA from control MSC with induction of BMP-2 (250 ng/ml, 3 days).

Fig. 8. Data quality check. Hierarchical clustering (left), and MDS plot (right).

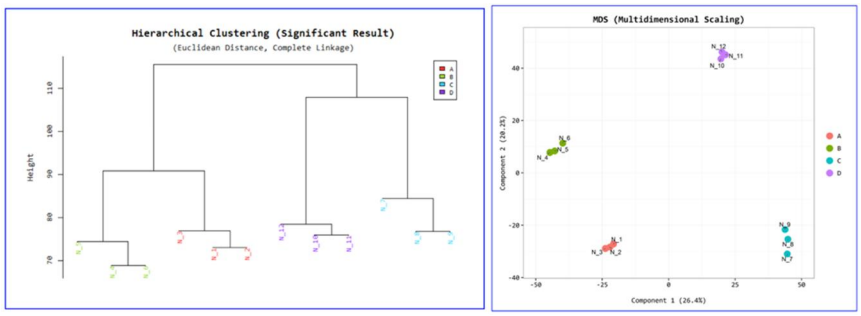

Relative gene expression level

Relative gene expression was compared between aging MSCs treated with and without rhBMP-2, between control MSCs treated with or without rhBMP-2, and between all four groups of cells. The numbers of up- and downregulated probes (absolute fold change (FC) ≥ 1.5 or 2, $P < 0.05$) are shown in Figure 9a. There were more upregulated genes in rhBMP-2-treated aging MSCs than in rhBMP-2-treated control MSCs and non-treated aging MSCs. The numbers of significantly up- and downregulated genes (absolute FC ≥ 1.5 or 2, $P < 0.05$) are presented in Figure 9b.

Fig. 9a. Up- and down regulated probes count by absolute fold change ≥ 1.5 or 2 in comparisons among various type of samples

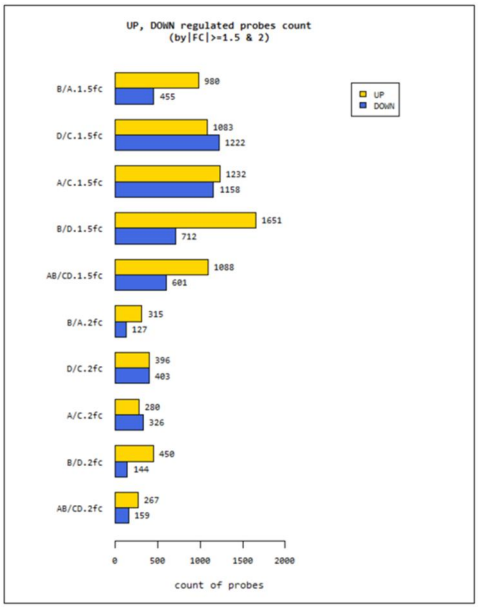

Fig. 9b. Significant probes count by absolute fold change ≥ 1.5 or 2, and *P* value < 0.05 in comparisons among various type of samples (bh. *P* value; adjusted *P* value by using Benjamini-Hochberg algorithm)

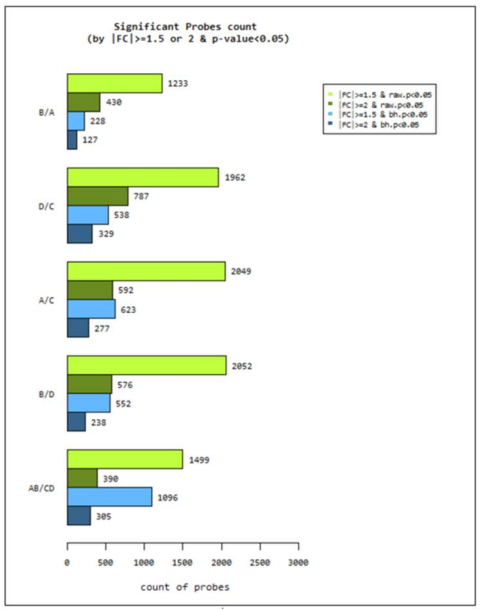

Volume plots of relative gene expression (signal intensity) are also provided (Fig. 10).

Fig. 10. Volume plots showing top 5 genes (red dots) with significant cut-off value (absolute fold change ≥ 1.5 and *P* value < 0.05) and higher volume

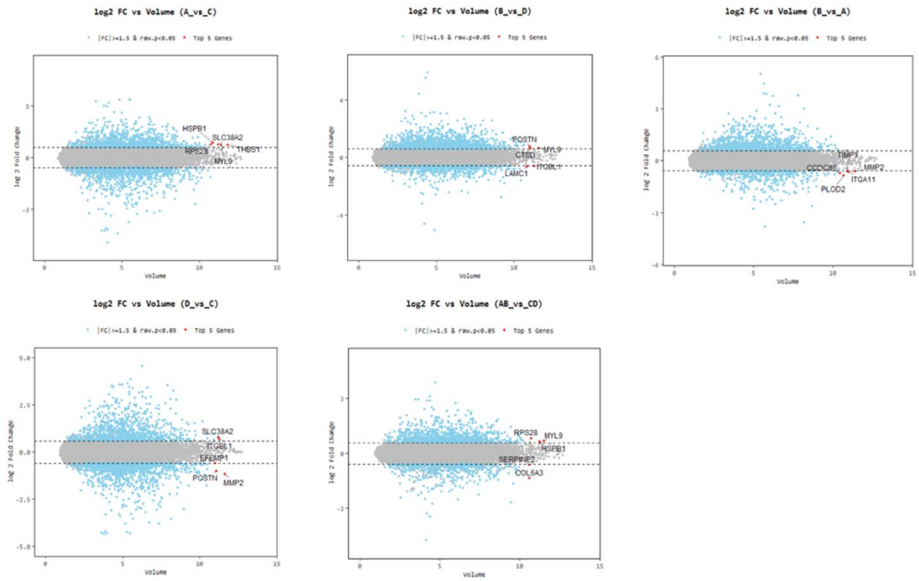

Gene-enrichment and functional annotation analysis

1. GSEA

1) Aging MSC without BMP-2 (phenotype A) vs. Aging MSC with BMP-2 (phenotype B)

(1) Aging related gene set: 1 enrichment for phenotype A vs 4 enrichments for phenotype B

Among 36 gene sets, 1 gene set (KAYO_AGING_MUSCLE_DN) is significantly enriched in phenotype 'Aging MSC without BMP-2, and 4 gene sets are enriched in phenotype 'Aging MSC with BMP-2'. More upregulated gene sets are observed by induction of BMP-2 in aging MSCs. Enrichment plots and heat maps for core enrichment are described in Fig. 11.

Fig. 11. Enrichment plot and heat map for core enrichment in phenotype ‘aging MSC without BMP-2’, and ‘aging MSC with BMP-2’ (Aging related gene set). Heat maps for ‘LEE_AGING_MUSCLE_UP’, and ‘RODWELL_AGING_KIDNEY_DN’ are not included for too many samples.

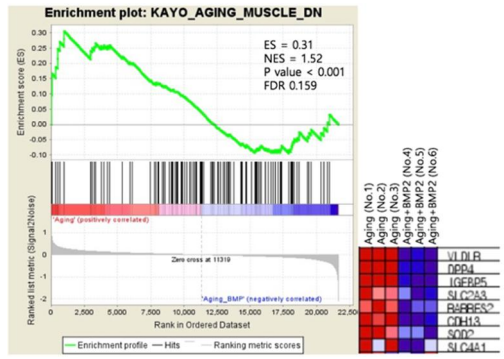

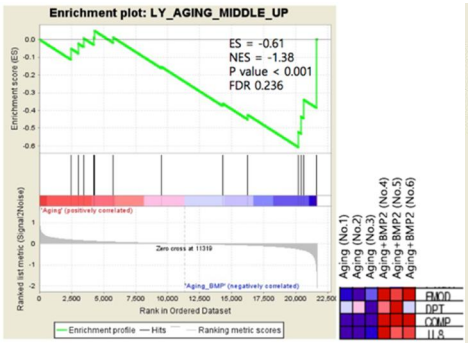

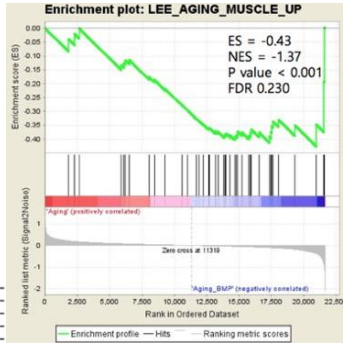

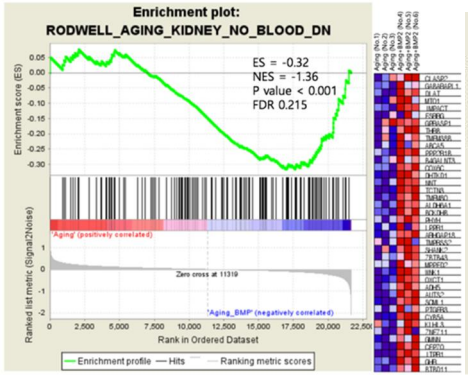

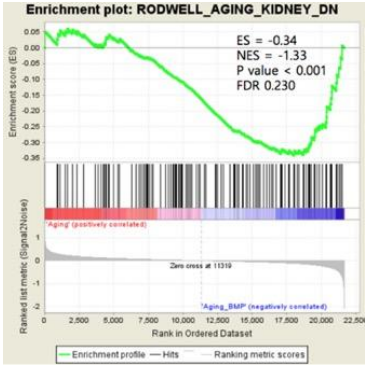

(2) BMP related gene set: No enrichment in phenotype A vs 4 enrichments for phenotype B

Among 5 gene sets, 4 gene sets are significantly enriched in phenotype ‘Aging MSC with BMP-2’. Enrichment plots and heat maps for core enrichment are described in Fig. 12.

Fig. 12. Enrichment plots and heat maps for core enrichment in phenotype ‘Aging MSC with BMP-2’. Heat maps in ‘LEE_BMP2_TARGETS_DN’ and ‘LEE_BMP2_TARGETS_UP’ are not included for its too many samples. (BMP related gene set)

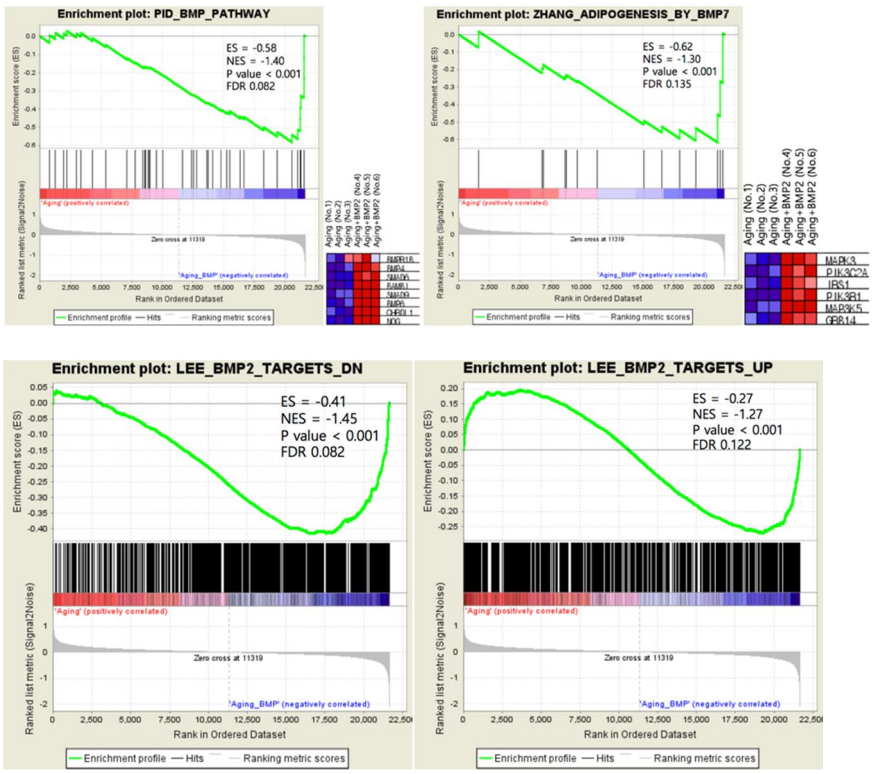

(3) Osteogenesis related gene set: 1 enrichment in phenotype A vs no enrichment for phenotype B

Among 3 gene sets, 1 gene set is significantly enriched in phenotype ‘Aging MSC without BMP-2’. Enrichment plot and heat map for core enrichment are described in Fig. 13.

Fig. 13. Enrichment plot and heat map for core enrichment in phenotype ‘Aging MSC without BMP-2’ (Osteogenesis related gene set)

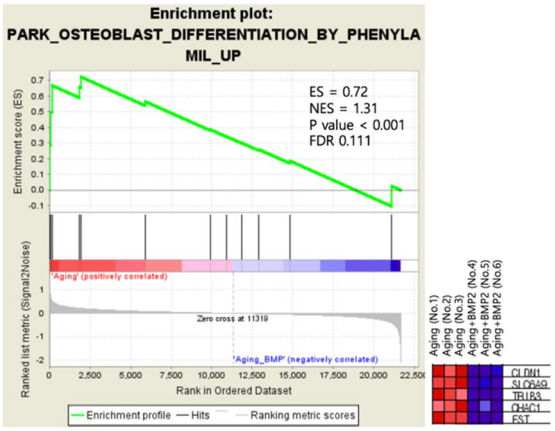

(4) Adipogenesis related gene set: 3 enrichments in phenotype A vs 22 enrichments for phenotype B

Among 44 gene sets, 3 gene sets are significantly enriched in phenotype ‘Aging MSC without BMP-2, and 22 gene sets are enriched in phenotype ‘Aging MSC with BMP-2’. More upregulated gene sets are observed by induction of BMP-2 in aging MSCs. Representative enrichment plots and heat maps for core enrichment are described in Fig. 14.

Fig. 14. Enrichment plot and heat map for core enrichment in phenotype ‘Aging MSC without BMP-2’ and ‘Aging MSC with BMP-2’. Only 2 representative gene sets in each phenotype are suggested. (Adipogenesis related gene set)

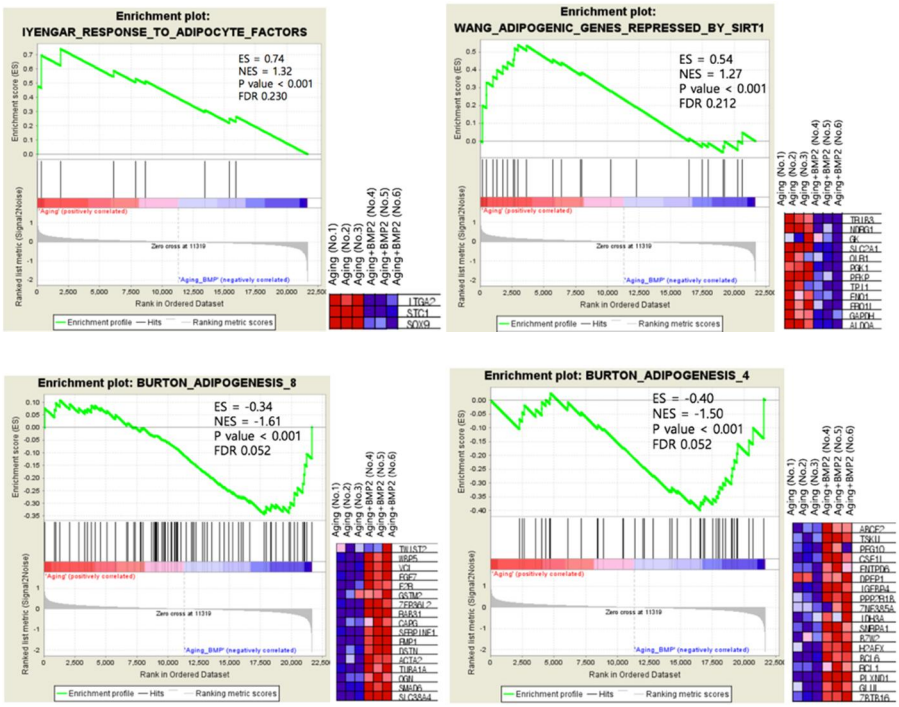

(5) Senescence related gene set: 1 enrichment in phenotype A vs no enrichment for phenotype B

Among 6 gene sets, 1 gene set is significantly enriched in phenotype ‘Aging MSC without BMP-2’. Enrichment plot and heat map for core enrichment are described in Fig. 15.

Fig. 15. Enrichment plot and heat map for core enrichment in phenotype ‘Aging MSC without BMP-2’ (Senescence related gene set)

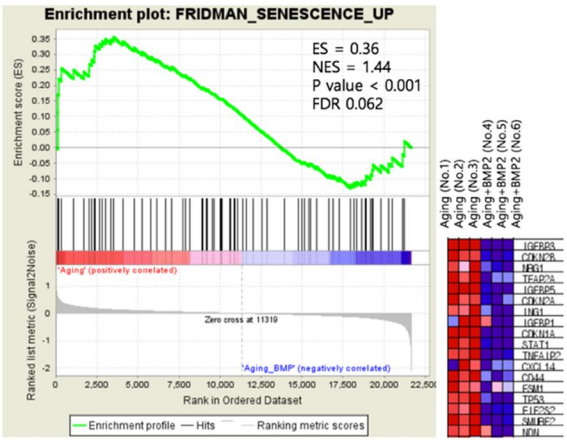

2) Control MSC without BMP-2 (sample C) vs. Control MSC with BMP-2 (sample D)

(1) Aging related gene set: 10 enrichments for phenotype C vs 1 enrichment for phenotype D

Among 36 gene sets, 10 gene set is significantly enriched in phenotype ‘Control MSC without BMP-2, and 1 gene set is enriched in phenotype ‘Control MSC with BMP-2’. Aging related gene sets are frequently downregulated by the induction of BMP-2 in young MSCs. Representative enrichment plots and heat maps for core enrichment are described in Fig. 16.

Fig. 16. Enrichment plot and heat map for core enrichment in phenotype ‘Control MSC without BMP-2’ and ‘Control MSC with BMP-2’. Only 1 representative gene set in each phenotype are suggested. (Aging related gene set)

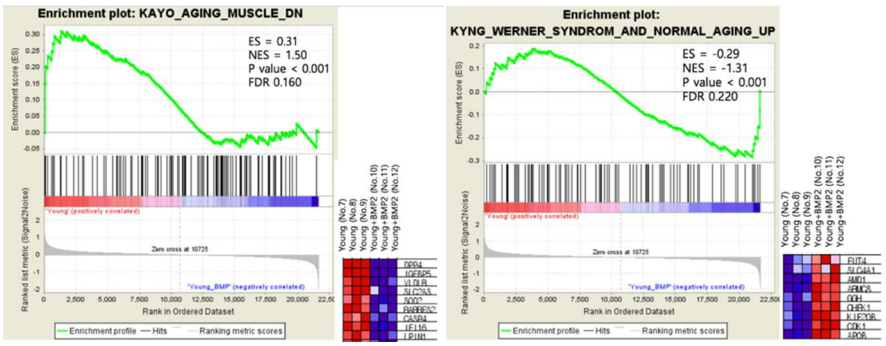

(2) BMP related gene set: 1 enrichment in phenotype C and D

Among 5 gene sets, 1 gene set is significantly enriched in each phenotype. Enrichment plots and heat maps for core enrichment are described in Fig. 17.

Fig. 17. Enrichment plots and heat maps for core enrichment in phenotype ‘Control MSC without BMP-2’ and ‘Control MSC with BMP-2’. Heat maps are not included for its too many samples. (BMP related gene set)

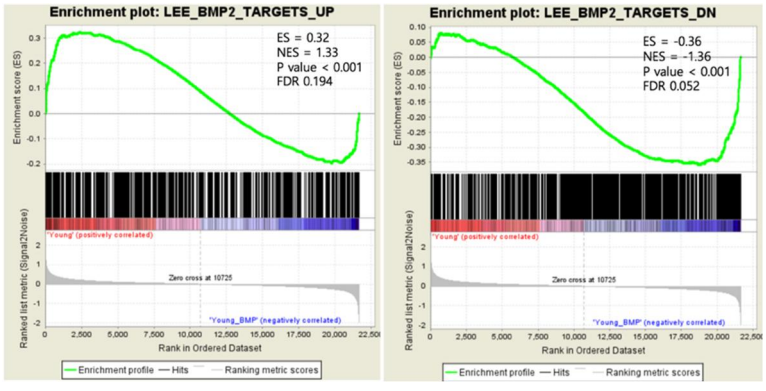

(3) Osteogenesis related gene set: no enrichment in each type

(4) Adipogenesis related gene set: 17 enrichments in phenotype C and D

Among 44 gene sets, 17 gene sets are significantly enriched in phenotype ‘Control MSC without BMP-2’, and another 17 gene sets are enriched in phenotype ‘Control MSC with BMP-2’. Enrichment plots and heat maps for core enrichment are skipped for its massive material.

(5) Senescence related gene set: 1 enrichment in phenotype C and 2 enrichments in phenotype D

Among 6 gene sets, 1 gene set is significantly enriched in phenotype ‘Control MSC without BMP-2’, and 2 gene sets are enriched in phenotype ‘Control MSC with BMP-2’. Enrichment plot and heat map for core enrichment are described in Fig. 18.

Fig. 18. Enrichment plot and heat map for core enrichment in phenotype ‘Control MSC without BMP-2’ and ‘Control MSC with BMP-2’ (Senescence related gene set)

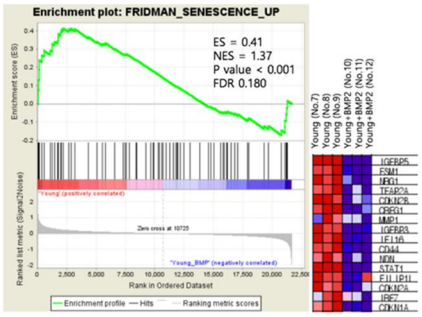

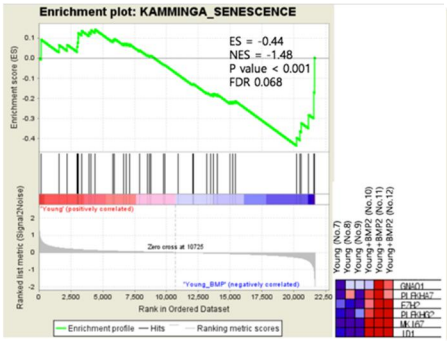

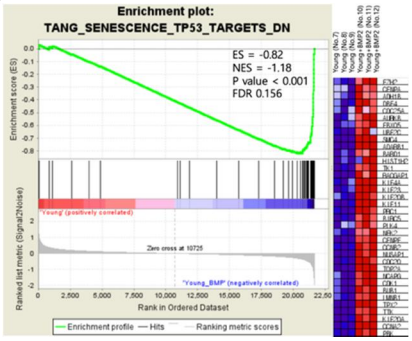

3) Control MSC (Sample CD) vs Aging MSC (Sample AB)

(1) Aging related gene set: no enrichment in phenotype CD and 1 enrichment in phenotype AB

Among 36 gene sets, 1 gene set (JIANG_AGING_HYPOTHALAMS_DN) is significantly enriched in phenotype ‘Aging MSC’. Enrichment plot and heat map for core enrichment are described in Fig. 19.

Fig. 19. Enrichment plot and heat map for core enrichment in phenotype ‘Aging MSC’ (Aging related gene set)

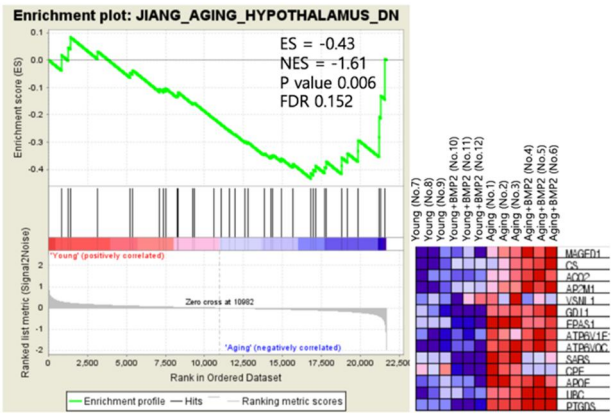

(2) BMP related gene set: no enrichment in each phenotype

(3) Osteogenesis related gene set: no enrichment in each phenotype

(4) Adipogenesis related gene set: 1 enrichment in phenotype CD and 4 enrichments in phenotype AB

Among 44 gene sets, 1 gene set is significantly enriched in phenotype ‘Control MSC’, and 4 gene sets are enriched in phenotype ‘Aging MSC’. Enrichment plots and heat maps for core enrichment are described in Fig. 20.

Fig. 20. Enrichment plots and heat maps for core enrichment in phenotype ‘Control MSC’ and ‘Aging MSC’. Heat maps are not included in ‘KEGG_ADIPOCYTOKINE_SIGNALING_PATHWAY’, ‘BURTON_ADIPOGENESIS_5’, and ‘BURTON_ADIPOGENESIS_8’. (Adipogenesis related gene set)

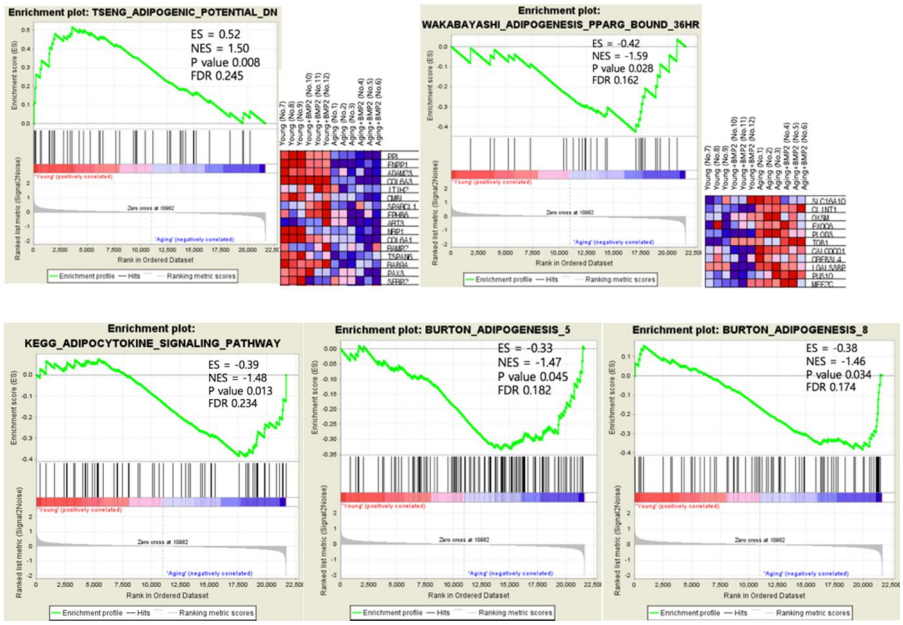

(5) Senescence related gene set: no enrichment in each phenotype

In short, overall numbers of upregulated gene sets and significant enrichment were compared in Table 2. Aging related gene sets were much more upregulated by the induction of BMP-2 in aging cells compared to control cells. Adipogenesis related gene sets were also more upregulated by the induction of BMP-2 in aging cells. This trend was also found in BMP related gene sets.

Table 2. The number of upregulated and significantly enriched gene sets in each phenotype

Phenotype	Gene sets	Number of gene sets	Upregulated gene sets	Significant enrichment*
A / B	Aging	36	11 / 25	1 / 4
C / D	Aging	36	20 / 16	10 / 1
CD / AB	Aging	36	13 / 23	0 / 1
A / B	BMP	5	0 / 5	0 / 4
C / D	BMP	5	3 / 2	1 / 1
CD / AB	BMP	5	1 / 4	0 / 0
A / B	Osteogenesis	3	1 / 2	1 / 0
C / D	Osteogenesis	3	3 / 0	0 / 0
CD / AB	Osteogenesis	3	1 / 2	0 / 0
A / B	Adipogenesis	44	11 / 33	3 / 22
C / D	Adipogenesis	44	20 / 24	17 / 17
CD / AB	Adipogenesis	44	15 / 29	1 / 4
A / B	Senescence	6	1 / 5	1 / 0
C / D	Senescence	6	3 / 3	1 / 2
CD / AB	Senescence	6	3 / 3	0 / 0

A: Aging MSC without BMP-2; B: Aging MSC with BMP-2; C: Control MSC without BMP-2; D: Control MSC with BMP-2

* FDR < 25% and nominal *P* value < 0.05

2. GSEA leading edge subset analysis for Control MSC (Sample CD) vs Aging MSC (Sample AB)

All results of leading edge subsets were proposed as heat maps in Fig. 21. Overlapped genes among different gene sets are not frequently found in osteogenesis, adipogenesis or senescence related gene sets. Overlapped genes more than 2 different gene sets were described in Fig. 22.

In aging related leading edge subsets, 64 clustered genes were upregulated in aging MSCs (blue color), and 49 clustered genes were upregulated in control MSCs (red color). In BMP related leading edge subsets, 6 clustered genes were upregulated in aging MSCs (blue color). They included CHRDL1 (chordin-like 1), NOG (noggin), SMAD1, SMAD7, FST (follistatin), and BAMBI (BMP and activin membrane-bound inhibitor homolog). These genes might be candidates for senescence dependent BMP-2 effect on differentiation of MSCs although they should be confirmed by real time PCR.

Fig. 21. Heat maps for leading edge subsets. Signals about aging, BMP, osteogenesis, adipogenesis, and senescence-related genes sets (from above to below)

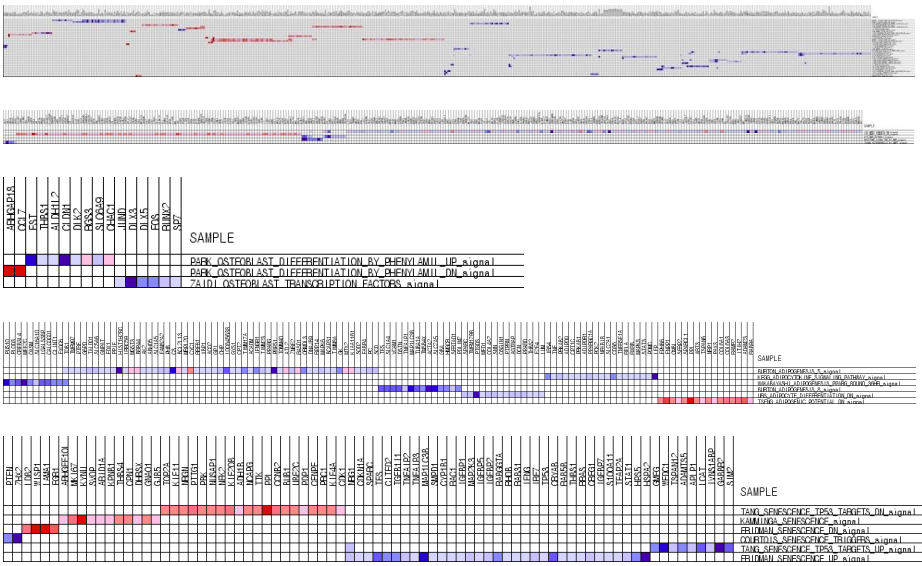

Fig. 22. Heat maps showing up- or down regulation in more than 2 gene sets in the leading edge subsets. (above) aging related gene sets (below) BMP related gene sets.

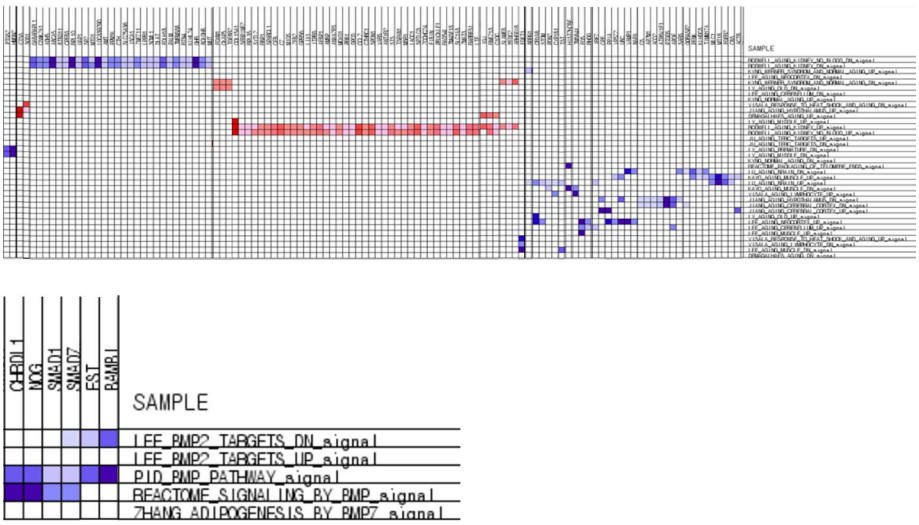

3. MetaCore analysis

1) Aging MSC with BMP-2 (sample B) vs. Aging MSC without BMP-2 (sample A)

The most relevant network was ‘p53, Brca1, IL-1RI, GADD45 beta, CDK2’, followed by ‘c-Myc, CDK1 (p34), Beta-catenin, PLK1, Tcf (Lef)’. These networks were illustrated in Fig. 23. Thick cyan lines indicate the fragments of canonical pathways. Up-regulated genes are marked with red circles; down-regulated with blue circles. The 'checkerboard' color indicates mixed expression for the gene between files or between multiple tags for the same gene. In aging MSCs, IL-1ß, IL-6, and NGF is upregulated by BMP-2 through NF-kB or p38 MAPK pathway.

Fig. 23. The top scored and second scored networks from aging MSC with BMP-2 vs aging MSC without BMP-2.

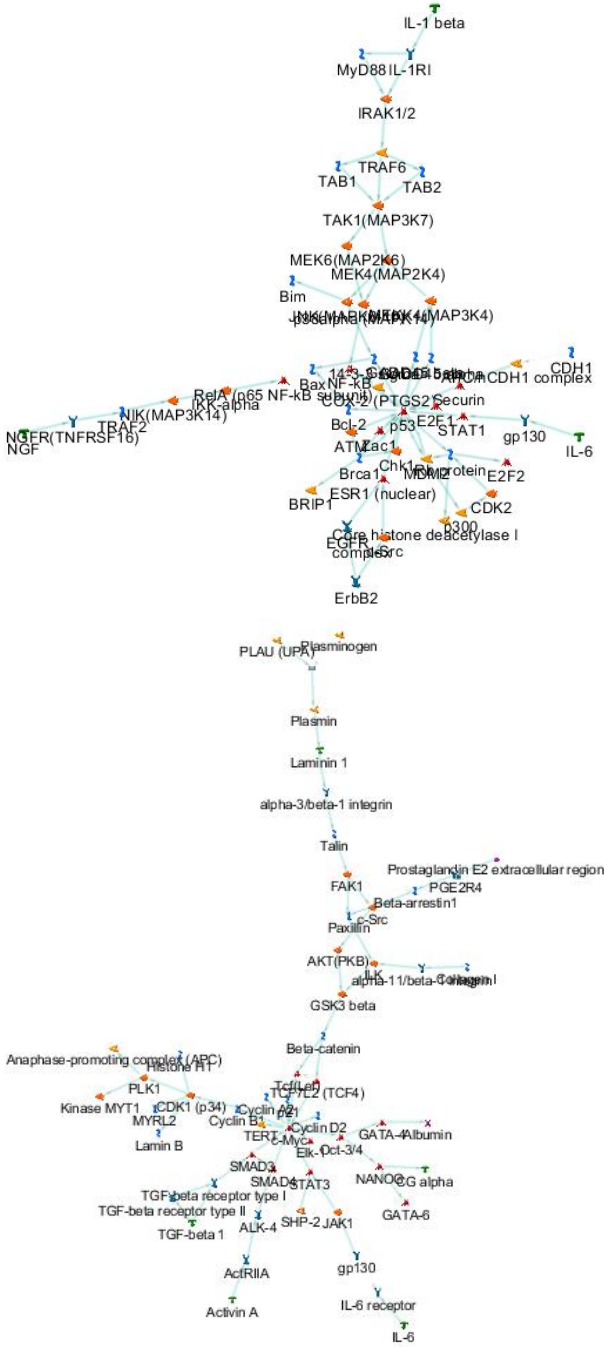

2) Control MSC with BMP-2 (sample D) vs. Control MSC without BMP-2

(sample C)

The most relevant network was ‘MMP-2, DAB2, ActRIIA, MEK6(MAP2K6), Versican’, followed by ‘PI3K reg class IA (p85), PI3K reg class IA, I-kB, NFKB1A, Neuregulin 1’. These networks were illustrated in Fig. 24. In young MSCs, TGF-beta, activin, and BMP4/6 are upregulated by BMP-2 through BMP/SMAD signaling pathway.

Fig. 24. The top scored and second scored networks from control MSC with BMP-2 vs control MSC without BMP-2

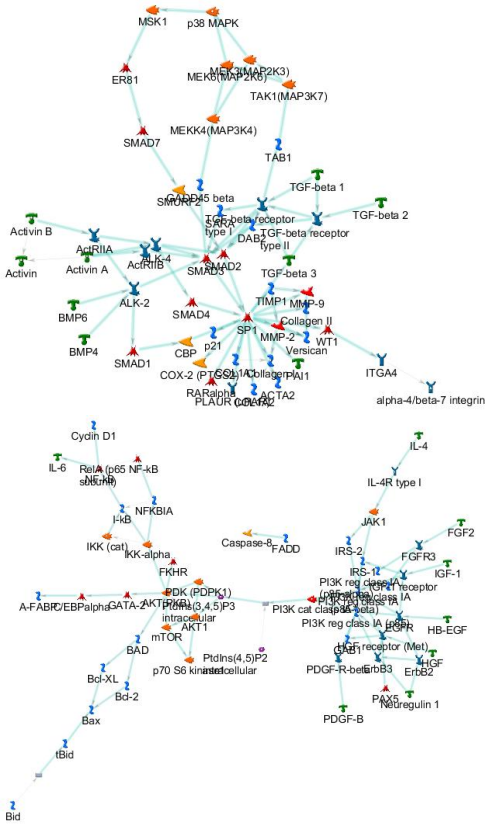

3) Aging MSC (sample AB) vs Control MSC (sample CD)

The most relevant network unique for aging MSCs was ‘PPAR-gamma, PKA-reg (cAMP-dependent), Leptin, PGE2R4, SCD’. However, the most relevant network for young MSCs was ‘Survivin, Caspase-3, I-kB, Apo-2L(TNFSF10), IGF-1’ (Fig. 25).

Fig. 25. The top scored network that unique for aging MSCs (above), and control MSC (below).

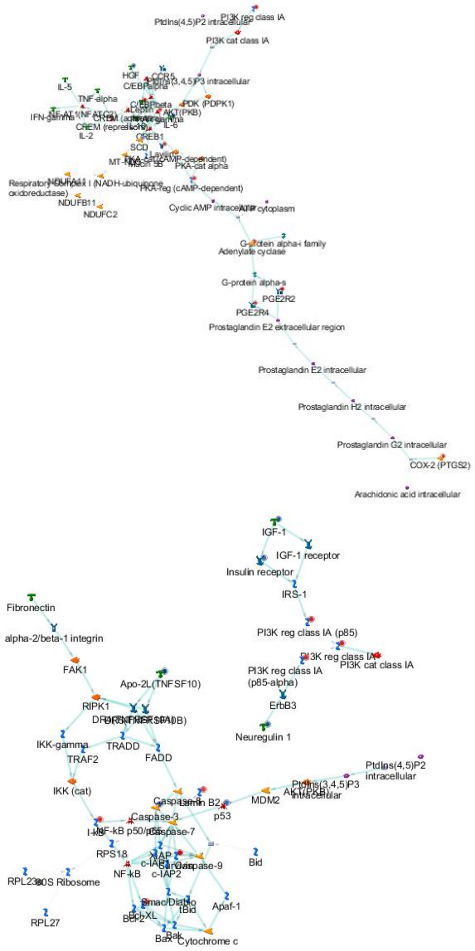

Discussion

In this study, we serially passaged MSCs in medium containing a high concentration of glucose to induce senescence. Cellular senescence is characterized by morphologic changes, telomere shortening, and doubling time lengthening (Bonab et al. 2006). Aging-related cellular senescence was first suggested by Hayflick (Hayflick 1965). Telomere shortening is proposed to be associated with decreased cellular proliferation (Baxter et al. 2004). Cellular senescence was previously induced via serial passage and the differentiation potential was suggested to decrease after six passages (Bonab et al. 2006). These results were confirmed by our findings that SA-β-gal staining and expression of senescence markers were increased in MSCs after six or seven passages. To ensure aging was induced, the medium was supplemented with a high concentration of glucose after the fourth passage. Treatment with a high concentration of glucose is proposed to induce replicative senescence via the Akt/mTOR pathway (Stolzing et al. 2006, Chang et al. 2015, Zhang et al. 2017).

We hypothesized that osteogenic and adipogenic differentiation upon BMP-2 stimulation would be lower and higher in aging MSCs than in control MSCs, respectively. A similar idea was previously suggested and verified. MSCs from young and old donors were reported to form similar levels of mineralized matrix in vitro and give rise to similar numbers of adipocytes, indicating that cellular senescence does not affect osteoblastic activity

(Stenderup et al. 2003). No age-related changes in gene expression of osteoblastic or adipogenic markers were observed in their previous study (Justesen et al. 2002). However, differentiation was not compared between aging and young MSCs stimulated with various concentrations of BMP-2. We found that osteogenic differentiation induced by BMP-2, as assessed by calcium assay, ALP activity and osteogenic marker expression, was decreased in aging MSCs, in agreement with our hypothesis.

The effect of aging on the bone inductive activity of BMP-2 has been researched in vitro and in vivo. Fleet et al. reported that bone formation scores following intraabdominal implantation of rhBMP-2 are lower in aging rats than in young rats and that this difference decreases as the concentration of rhBMP-2 increases (Fleet et al. 1996). Another study demonstrated that the bone mineral content, bone area, and bone mineral density decrease with aging in rats (Hara et al. 2015). However, these studies did not analyze adipogenic differentiation. mRNA expression of adipogenic lineage markers such as aP2 is reportedly higher in old mice than in adult mice (Moerman et al. 2004). This is supported by the suggestion that the osteogenic and adipogenic potentials of MSCs derived from aged rats are lower and higher than those derived from young rats, respectively (Abuna et al. 2016). However, several studies reported that aging decreases the adipogenic differentiation potential of MSCs (Bonab et al. 2006, Wagner et al. 2008, Cheng et al. 2010). They proposed that replicative senescence increases osteogenic differentiation of MSCs on the basis of increased ARS staining and ALP activity (Wagner et al.

2008, Cheng et al. 2010). However, this does not explain why osteogenesis decreases with aging. Furthermore, the effect of BMP-2 stimulation was not considered. Our finding that osteogenic differentiation was reduced in aging MSCs disputes these results and explains why bone formation decreases with aging. In addition, the adipogenic differentiation potential did not differ between aging and control MSCs, which means relative overexpression of adipogenesis with aging process.

rhBMP-2 induced osteogenic differentiation of aging MSCs in a dose-dependent manner. ALP activity in aging MSCs treated with 250 ng/ml rhBMP-2 was comparable to that in control MSCs treated with 25 ng/ml rhBMP-2 after 7 days. In addition, aging MSCs treated with 500 ng/ml rhBMP-2 released a comparable amount of Ca^{2+} as control MSCs treated with 100 ng/ml BMP-2. Consequently, aging MSCs treated with a high concentration of BMP-2 might demonstrate comparable osteogenic activity as control MSCs.

The effect of BMP-2 on differentiation of aging MSCs is unclear. One study reported that BMP-2 production by MSCs from rats of various ages does not differ following BMP-2 gene transduction, indicating that this transduction restores the osteogenic potential of MSCs (Yue et al. 2005). However, this result cannot support the maintenance of osteogenic potential in aging MSCs by the stimulation of exogenous BMP-2. It was recently reported that the capacity of exogenous BMP-2 to induce osteogenesis decreases with age (Hara et al. 2015). Our study supports this finding, although treatment with a

high concentration of rhBMP-2 still induced osteogenesis of aging MSCs.

The concentration of BMP-2 may influence the signaling pathways that control osteogenic and adipogenic differentiation. It was suggested that treatment with low and high concentrations of BMP-2 induces adipogenic and osteogenic differentiation of MSCs, respectively (Wang et al. 1993). However, the concentration-dependent effects of BMP-2 might be complicated. BMP receptor (BMPR) specific signaling pathways have been proposed although no general rule can be applied. Signaling via BMPR-1A induces adipogenesis, while signaling via BMPR-1B induces osteogenesis in a rodent cell line (Chen et al. 1998, James 2013). Extensive cross-talk occurs between the signaling pathways that control the differentiation of human MSCs (Bilem et al. 2016, Zhuang et al. 2016). Unfortunately, the current study did not determine whether MSCs preferentially undergo osteogenic or adipogenic differentiation according to the concentration of BMP-2. Treatment with rhBMP-2 increased both types of differentiation in a dose-dependent manner. However, decreased osteogenic, and increased adipogenic differentiation by the BMP-2 stimulation in aging MSCs could be presumed by several aspects. Ca^{2+} release was comparable in aging and control MSCs upon treatment with 25 ng/ml rhBMP-2, whereas it was markedly lower in the former cells than in the latter cells upon treatment with concentrations of rhBMP-2 higher than 100 ng/ml. However, there was no difference between aging and control MSCs in the adipogenesis assay. In addition, treatment with a high concentration of rhBMP-2 did not increase mRNA expression of Runx2, BSP, or OCN in aging

MSCs. However, rhBMP-2 dose-dependently increased expression of PPARγ, which is considered the most important transcription factor for adipogenesis. Therefore, treatment with a high concentration of BMP-2 might favor adipogenic differentiation.

Changes to the proliferative capacity may underlie why osteogenesis of MSCs decreases with aging. The number of BM-derived MSCs with osteogenic potential was reported to decrease at an early stage of aging (D'Ippolito et al. 1999). This is supported by the findings that aging decreases the number of osteoprogenitor cells in a mouse model and the growth of these cells in BM stromal cell cultures (Chen 2004). However, another study proposed that the number and proliferative capacity of osteoprogenitor cells are maintained during aging in humans (Stenderup et al. 2001).

The expression levels of many genes can be investigated simultaneously via microarray analysis (Menicanin et al. 2009). Several microarray analyses of gene expression during BMP-2-induced differentiation of MSCs have been reported (Vaes et al. 2002, de Jong et al. 2004); however, such analyses have not been conducted to compare senescent and non-senescent MSCs. We performed microarray analysis of MSCs treated with 250 ng/ml rhBMP-2 for 3 days. This is because mRNA expression of osteogenic markers, such as ALP and BSP, markedly differed between MSCs treated with 100 ng/ml rhBMP-2 and those treated with 250 ng/ml rhBMP-2 as well as between two cells showed dramatic differences in 7 days. Consequently, there would be an enormous number of differentially expressed genes in cells cultured for 7 days.

Instead, we investigated early changes in gene expression by analyzing cells after 3 days.

Multidimensional scaling showed regular character of each type of samples (Fig. 8). Among more than 40,000 probes, about 10% significantly differed in at least one comparison. The numbers of up- and downregulated probes most dramatically differed in the comparison of rhBMP-2-treated aging and control MSCs (Fig. 9). There were 2–3-fold more upregulated probes than downregulated probes in rhBMP-2-treated aging MSCs vs. rhBMP-2-treated control MSCs. A similar difference was observed in the comparison of rhBMP-2-treated and non-treated aging MSCs. However, the numbers of up- and downregulated probes were similar in the comparison of non-treated aging and control MSCs. So, it is thought that more upregulated genes could be derived by the induction of BMP-2 especially in aging cells.

The result of GSEA and MetaCore analysis revealed a few important findings regardless of difficult interpretation due to their complexity. The number of upregulated, and significantly enriched gene sets showed aging and adipogenesis related gene sets were upregulated by BMP-2 in aging MSCs (Table 2). In addition, 6 genes (CHRDL1, NOG, SMAD1, SMAD7, FST, and BAMBI) in BMP related gene sets were upregulated in aging MSCs based on leading edge subset analysis (Fig. 23). It was reported that chordin-like protein 1 (CHRDL1) showed strong correlation with chronological age (Menni et al. 2015). Furthermore, it was known as BMP-2/-4 antagonist like

noggin (Talavera-Adame et al. 2013). Enhanced osteogenesis by suppression of noggin with BMP-2 was also suggested (Albers et al. 2012, Fan et al. 2013). Smad1 is one of regulatory Smad (R-Smad), which mediates multiple signaling pathways including Smad-Runx2 pathway. However, Smad1 is known to enhance PPARγ, a key transcription factor for adipocyte differentiation (Jin et al. 2006). Whereas, Smad7 is an inhibitory Smad (I-Smad) to inhibit signal transduction in Smad-Runx2 pathway (Zhang et al. 2007). Knock down Smad7 mRNA revealed bone formation by increased R-Smad transcription (Layliev et al. 2013). However, role of Smad signaling in adipocyte differentiation has been controversial. Smad7 inhibits TGF-ß signal, which may promote adipogenesis and induce C/EBP transactivation (Choy et al. 2003). However, Smad7 was also proposed as negative regulators of adipogenesis regardless of its inhibitory effect of TGF-ß (Choy et al. 2000). Complex cross-talk might exist Smad signaling pathways. Follistatin (FST) was also reported to be crucial for adipocyte differentiation (Flanagan et al. 2009). It was also proposed that activin A:FST ratio is important to determine differentiation of a mesenchymal progenitor cell line into osteoblasts and adipocytes (Kawabata et al. 2007). However, BAMBI has been understood as a potent negative regulator of adipogenesis although they were mouse and porcine model (Luo et al. 2012, Mai et al. 2014). So, upregulation of BAMBI by BMP-2 in aging MSCs in the current study are not well understood based on previous studies.

Unique signaling pathways in various comparisons could be found by

MataCore analysis. Interestingly, signaling pathways induced by BMP-2 were different between aging and young MSCs. In young MSCs, BMP, SMAD, and activin are correlated, and make relevant networks. This means osteogenesis related pathway is upregulated by BMP-2 in young MSCs. Activin was reported to enhance bone healing property by using activing A/BMP2 chimera (Yoon et al. 2014, Zheng et al. 2017). In contrast, IL-1ß, IL-6, or NGF (nerve growth factor) is upregulated by BMP-2 in aging MSCs, and NF-kB or p38 MAPK pathway might be important. In fact, NF-kB is a proinflammatory master switch to upregulate important inflammatory factors such as IL-6 (Jain et al. 1999). NF-kB signaling is also reported to have an antagonistic effect in differentiation of MSCs into adipocytes (Cortez et al. 2013, Wang et al. 2013). So, activation of NF-kB pathway could mean inhibition of adipogenic differentiation even in aging MSCs. P38 MAPK is involved in cell differentiation, apoptosis and autophagy, which is persistently activated by ageing (Segales et al. 2016). P38 MAPK also plays a positive role in human adipogenesis by regulation of C/EBPß and PPARγ (Aouadi et al. 2007). Several reports revealed downregulation of p38 MAPK signaling inhibits MSCs commitment to adipocytes (Kim et al. 2010, Lee et al. 2011, Wilde et al. 2016). It is not likely to explain the difference of MSC differentiation by simple relevant pathway due to complex cross-talk mechanisms. However, the effect of BMP-2 on differentiation of MSCs could be different according to cellular aging based on the result of this study although some conflicting evidences have been reported.

The BMP-2 effect of aging on bone formation or bone fusion in clinical areas have not been well established. The new bone volume by BMP-2 combined with a fibrous collagen membrane (FCM) did not differ among the different age groups in rats (Matsumoto et al. 2001). However, it was also reported that bone formation by BMP-2 decreases with aging in rats (Hara et al. 2015). In the human study, it was proposed that the fusion rate and fusion time by rhBMP-2 were significantly better in patients <65 years of age than in patients >65 years of age (Lee et al. 2010). This is also supported by our study showing the differentiation of MSC by BMP-2 favors adipogenesis over osteogenesis. However, the result of in vitro study does not guarantee the same result of in vivo study. We only analyzed MSCs by replicative senescence. In fact, MSCs from old animals did not contain 100% of senescence cells. The proportion of senescence cells between young and old bone marrow MSCs were about 20% and 30% respectively (Beane et al. 2014). In addition, no differences of senescence cells were found by aging in adipose derived stem cells (Beane et al. 2014). In this respect, the difference of BMP-2 effect on differentiation of MSCs could not easily revealed in vivo study.

This study has several limitations. First, we focused on osteogenic and adipogenic differentiation; however, MSCs can differentiate into cells of other mesenchymal lineages such as chondrocytes and myocytes (Galli et al. 2014, Somoza et al. 2014). However, osteogenesis and adipogenesis is generally regarded as the most important crosstalk mechanism in differentiation of

MSCs (Abdallah et al. 2012, Zhuang et al. 2016). Second, this is an in vitro study and the results should be confirmed in animals or humans to facilitate the therapeutic use of BMP-2. A recent review highlighted that the effect of aging on the differentiation of MSCs in vivo is unclear (Khan et al. 2016). Third, the results of GSEA and MetaCore analysis did not reveal commonly related genes, which leaves much to be desired. Despite these limitations, this study is the first study to compare the effects of various concentrations of rhBMP-2 on the differentiation of aging and young bone marrow MSCs, and to investigate the candidate genes and involved signaling pathways by microarray analyses.

Conclusion

In conclusion, aging MSCs showed less osteogenic differentiation and comparable adipogenic differentiation in response to BMP-2 compared to control MSCs. The relative differentiation of aging MSCs toward osteogenic lineage compared to adipogenic lineage could be decreased by higher concentration of BMP-2. Relative superior adipogenic differentiation by BMP-2 in aging MSCs is supported by the result of microarray analysis. In addition, several genes might be candidates for senescence dependent BMP-2 effect on differentiation of MSCs although these genes should be confirmed in further real-time PCR. Different signaling pathway might play a role in different response to BMP-2 between aging and young MSCs. Further in vivo research along with the current study may contribute to effective use of BMP-2 in clinical fields by elucidating the signaling pathway whether MSCs differentiate into osteoblasts or adipocytes by BMP-2.

References

Abdallah BM, Kassem M: New factors controlling the balance between osteoblastogenesis and adipogenesis. **Bone 50:**540-545, 2012

Abuna RP, Stringhetta-Garcia CT, Fiori LP, Dornelles RC, Rosa AL, Beloti MM: Aging impairs osteoblast differentiation of mesenchymal stem cells grown on titanium by favoring adipogenesis. **J Appl Oral Sci 24:**376-382, 2016

Akune T, Ohba S, Kamekura S, Yamaguchi M, Chung UI, Kubota N, et al: PPARgamma insufficiency enhances osteogenesis through osteoblast formation from bone marrow progenitors. **J Clin Invest 113:**846-855, 2004

Albers CE, Hofstetter W, Sebald HJ, Sebald W, Siebenrock KA, Klenke FM: L51P - A BMP2 variant with osteoinductive activity via inhibition of Noggin. **Bone 51:**401-406, 2012

Aouadi M, Jager J, Laurent K, Gonzalez T, Cormont M, Binetruy B, et al: p38MAP Kinase activity is required for human primary adipocyte differentiation. **FEBS Lett 581:**5591-5596, 2007

Bae HW, Rajaee SS, Kanim LE: Nationwide trends in the surgical management of lumbar spinal stenosis. **Spine (Phila Pa 1976) 38:**916-926, 2013

Baxter MA, Wynn RF, Jowitt SN, Wraith JE, Fairbairn LJ, Bellantuono I: Study of telomere length reveals rapid aging of human marrow stromal cells following in vitro expansion. **Stem Cells 22:**675-682, 2004

Beane OS, Fonseca VC, Cooper LL, Koren G, Darling EM: Impact of aging

on the regenerative properties of bone marrow-, muscle-, and adipose-derived mesenchymal stem/stromal cells. **PLoS One 9:**e115963, 2014

Berendsen AD, Olsen BR: Regulation of adipogenesis and osteogenesis in mesenchymal stem cells by vascular endothelial growth factor A. **J Intern Med 277:**674-680, 2015

Bilem I, Chevallier P, Plawinski L, Sone ED, Durrieu MC, Laroche G: RGD and BMP-2 mimetic peptide crosstalk enhances osteogenic commitment of human bone marrow stem cells. **Acta Biomater 36:**132-142, 2016

Bonab MM, Alimoghaddam K, Talebian F, Ghaffari SH, Ghavamzadeh A, Nikbin B: Aging of mesenchymal stem cell in vitro. **BMC Cell Biol 7:**14, 2006

Bosch J, Houben AP, Radke TF, Stapelkamp D, Bunemann E, Balan P, et al: Distinct differentiation potential of "MSC" derived from cord blood and umbilical cord: are cord-derived cells true mesenchymal stromal cells? **Stem Cells Dev 21:**1977-1988, 2012

Byun MR, Kim AR, Hwang JH, Kim KM, Hwang ES, Hong JH: FGF2 stimulates osteogenic differentiation through ERK induced TAZ expression. **Bone 58:**72-80, 2014

Chamberlain G, Fox J, Ashton B, Middleton J: Concise review: mesenchymal stem cells: their phenotype, differentiation capacity, immunological features, and potential for homing. **Stem Cells 25:**2739-2749, 2007

Chang TC, Hsu MF, Wu KK: High Glucose Induces Bone Marrow-Derived Mesenchymal Stem Cell Senescence by Upregulating Autophagy. **PLoS ONE 10:**e0126537, 2015

Chang TW: Binding of cells to matrixes of distinct antibodies coated on solid surface. **J Immunol Methods 65:**217-223, 1983

Chen D, Ji X, Harris MA, Feng JQ, Karsenty G, Celeste AJ, et al: Differential roles for bone morphogenetic protein (BMP) receptor type IB and IA in differentiation and specification of mesenchymal precursor cells to osteoblast and adipocyte lineages. **J Cell Biol 142:**295-305, 1998

Chen TL: Inhibition of growth and differentiation of osteoprogenitors in mouse bone marrow stromal cell cultures by increased donor age and glucocorticoid treatment. **Bone 35:**83-95, 2004

Cheng H, Qiu L, Ma J, Zhang H, Cheng M, Li W, et al: Replicative senescence of human bone marrow and umbilical cord derived mesenchymal stem cells and their differentiation to adipocytes and osteoblasts. **Mol Biol Rep 38:**5161-5168, 2011

Cho JH, Lee JH, Yeom JS, Chang BS, Yang JJ, Koo KH, et al: Efficacy of Escherichia coli-derived recombinant human bone morphogenetic protein-2 in posterolateral lumbar fusion: an open, active-controlled, randomized, multicenter trial. **Spine J 17:**1866-1874, 2017

Choy L, Derynck R: Transforming growth factor-beta inhibits adipocyte differentiation by Smad3 interacting with CCAAT/enhancer-binding protein (C/EBP) and repressing C/EBP transactivation function. **J Biol Chem 278:**9609-9619, 2003

Choy L, Skillington J, Derynck R: Roles of autocrine TGF-beta receptor and Smad signaling in adipocyte differentiation. **J Cell Biol 149:**667-682, 2000

Coomes AM, Mealey BL, Huynh-Ba G, Barboza-Arguello C, Moore WS,

Cochran DL: Buccal bone formation after flapless extraction: a randomized, controlled clinical trial comparing recombinant human bone morphogenetic protein 2/absorbable collagen carrier and collagen sponge alone. **J Periodontol 85:**525-535, 2014

Cortez M, Carmo LS, Rogero MM, Borelli P, Fock RA: A high-fat diet increases IL-1, IL-6, and TNF-alpha production by increasing NF-kappaB and attenuating PPAR-gamma expression in bone marrow mesenchymal stem cells. **Inflammation 36:**379-386, 2013

Crane JL, Zhao L, Frye JS, Xian L, Qiu T, Cao X: IGF-1 Signaling is Essential for Differentiation of Mesenchymal Stem Cells for Peak Bone Mass. **Bone Res 1:**186-194, 2013

D'Ippolito G, Schiller PC, Ricordi C, Roos BA, Howard GA: Age-related osteogenic potential of mesenchymal stromal stem cells from human vertebral bone marrow. **J Bone Miner Res 14:**1115-1122, 1999

de Jong DS, Vaes BL, Dechering KJ, Feijen A, Hendriks JM, Wehrens R, et al: Identification of novel regulators associated with early-phase osteoblast differentiation. **J Bone Miner Res 19:**947-958, 2004

Dingwall M, Marchildon F, Gunanayagam A, Louis CS, Wiper-Bergeron N: Retinoic acid-induced Smad3 expression is required for the induction of osteoblastogenesis of mesenchymal stem cells. **Differentiation 82:**57-65, 2011

Donoso O, Pino AM, Seitz G, Osses N, Rodríguez JP: Osteoporosis-associated alteration in the signalling status of BMP-2 in human MSCs under adipogenic conditions. **J Cell Biochem 116:**1267-1277, 2015

Fan J, Park H, Tan S, Lee M: Enhanced osteogenesis of adipose derived stem cells with Noggin suppression and delivery of BMP-2. **PLoS One 8:**e72474, 2013

Flanagan JN, Linder K, Mejhert N, Dungner E, Wahlen K, Decaunes P, et al: Role of follistatin in promoting adipogenesis in women. **J Clin Endocrinol Metab 94:**3003-3009, 2009

Fleet JC, Cashman K, Cox K, Rosen V: The effects of aging on the bone inductive activity of recombinant human bone morphogenetic protein-2. **Endocrinology 137:**4605-4610, 1996

Fontaine C, Cousin W, Plaisant M, Dani C, Peraldi P: Hedgehog signaling alters adipocyte maturation of human mesenchymal stem cells. **Stem Cells 26:**1037-1046, 2008

Fotia C, Massa A, Boriani F, Baldini N, Granchi D: Prolonged exposure to hypoxic milieu improves the osteogenic potential of adipose derived stem cells. **J Cell Biochem 116:**1442-1453, 2015

Galli D, Vitale M, Vaccarezza M: Bone marrow-derived mesenchymal cell differentiation toward myogenic lineages: facts and perspectives. **Biomed Res Int 2014:**762695, 2014

Gregory CA, Ylostalo J, Prockop DJ: Adult bone marrow stem/progenitor cells (MSCs) are preconditioned by microenvironmental "niches" in culture: a two-stage hypothesis for regulation of MSC fate. **Sci STKE 2005:**pe37, 2005

Hara T, Kakudo N, Morimoto N, Horio O, Ogura T, Kusumoto K: Effect of aging on the osteoinductive activity of recombinant human bone morphogenetic protein-2 in rats. **J Surg Res 195:**377-383, 2015

Hayflick L: THE LIMITED IN VITRO LIFETIME OF HUMAN DIPLOID CELL STRAINS. **Exp Cell Res 37:**614-636, 1965

Im GI, Shin YW, Lee KB: Do adipose tissue-derived mesenchymal stem cells have the same osteogenic and chondrogenic potential as bone marrow-derived cells? **Osteoarthritis Cartilage 13:**845-853, 2005

Jain RG, Phelps KD, Pekala PH: Tumor necrosis factor-alpha initiated signal transduction in 3T3-L1 adipocytes. **J Cell Physiol 179:**58-66, 1999

James AW: Review of Signaling Pathways Governing MSC Osteogenic and Adipogenic Differentiation. **Scientifica 2013:** 684736, 2013

Jin W, Takagi T, Kanesashi SN, Kurahashi T, Nomura T, Harada J, et al: Schnurri-2 controls BMP-dependent adipogenesis via interaction with Smad proteins. **Dev Cell 10:**461-471, 2006

Justesen J, Stenderup K, Eriksen EF, Kassem M: Maintenance of osteoblastic and adipocytic differentiation potential with age and osteoporosis in human marrow stromal cell cultures. **Calcif Tissue Int 71:**36-44, 2002

Kamiya N, Ye L, Kobayashi T, Lucas DJ, Mochida Y, Yamauchi M, et al: Disruption of BMP signaling in osteoblasts through type IA receptor (BMPRIA) increases bone mass. **J Bone Miner Res 23:**2007-2017, 2008

Kato S, Kawabata N, Suzuki N, Ohmura M, Takagi M: Bone morphogenetic protein-2 induces the differentiation of a mesenchymal progenitor cell line, ROB-C26, into mature osteoblasts and adipocytes. **Life Sci 84:**302-310, 2009

Kawabata N, Kamiya N, Suzuki N, Matsumoto M, Takagi M: Changes in extracellular activin A:follistatin ratio during differentiation of a mesenchymal progenitor cell line, ROB-C26 into osteoblasts and adipocytes. **Life Sci 81:**8-

18, 2007

Khan H, Mafi P, Mafi R, Khan W: The effects of ageing on differentiation and characterisation of human mesenchymal stem cells. **Curr Stem Cell Res Ther**, 2016

Kim KJ, Lee OH, Lee BY: Fucoidan, a sulfated polysaccharide, inhibits adipogenesis through the mitogen-activated protein kinase pathway in 3T3-L1 preadipocytes. **Life Sci 86:**791-797, 2010

Layliev J, Sagebin F, Weinstein A, Marchac A, Szpalski C, Saadeh PB, et al: Percutaneous gene therapy heals cranial defects. **Gene Ther 20:**922-929, 2013

Lee JS, Park JH, Kwon IK, Lim JY: Retinoic acid inhibits BMP4-induced C3H10T1/2 stem cell commitment to adipocyte via downregulating Smad/p38MAPK signaling. **Biochem Biophys Res Commun 409:**550-555, 2011

Lee KB, Taghavi CE, Hsu MS, Song KJ, Yoo JH, Keorochana G, et al: The efficacy of rhBMP-2 versus autograft for posterolateral lumbar spinal fusion in elderly patients. **Eur Spine J 19:**924-930, 2010

Luo X, Hutley LJ, Webster JA, Kim YH, Liu DF, Newell FS, et al: Identification of BMP and activin membrane-bound inhibitor (BAMBI) as a potent negative regulator of adipogenesis and modulator of autocrine/paracrine adipogenic factors. **Diabetes 61:**124-136, 2012

Mai Y, Zhang Z, Yang H, Dong P, Chu G, Yang G, et al: BMP and activin membrane-bound inhibitor (BAMBI) inhibits the adipogenesis of porcine preadipocytes through Wnt/beta-catenin signaling pathway. **Biochem Cell**

Biol 92:172-182, 2014

Matsumoto A, Yamaji K, Kawanami M, Kato H: Effect of aging on bone formation induced by recombinant human bone morphogenetic protein-2 combined with fibrous collagen membranes at subperiosteal sites. **J Periodontal Res 36:**175-182, 2001

Matsumoto S, Hayashi M, Suzuki Y, Suzuki N, Maeno M, Ogiso B: Calcium ions released from mineral trioxide aggregate convert the differentiation pathway of C2C12 cells into osteoblast lineage. **J Endod 39:**68-75, 2013

Menicanin D, Bartold PM, Zannettino AC, Gronthos S: Genomic profiling of mesenchymal stem cells. **Stem Cell Rev 5:**36-50, 2009

Menni C, Kiddle SJ, Mangino M, Vinuela A, Psatha M, Steves C, et al: Circulating Proteomic Signatures of Chronological Age. **J Gerontol A Biol Sci Med Sci 70:**809-816, 2015

Moerman EJ, Teng K, Lipschitz DA, Lecka-Czernik B: Aging activates adipogenic and suppresses osteogenic programs in mesenchymal marrow stroma/stem cells: the role of PPAR-gamma2 transcription factor and TGF-beta/BMP signaling pathways. **Aging Cell 3:**379-389, 2004

Pei L, Tontonoz P: Fat's loss is bone's gain. **J Clin Invest 113:**805-806, 2004

Pino AM, Rosen CJ, Rodriguez JP: In osteoporosis, differentiation of mesenchymal stem cells (MSCs) improves bone marrow adipogenesis. **Biol Res 45:**279-287, 2012

Plaisant M, Fontaine C, Cousin W, Rochet N, Dani C, Peraldi P: Activation of hedgehog signaling inhibits osteoblast differentiation of human mesenchymal stem cells. **Stem Cells 27:**703-713, 2009

Rippo MR, Babini L, Prattichizzo F, Graciotti L, Fulgenzi G, Tomassoni Ardori F, et al: Low FasL levels promote proliferation of human bone marrow-derived mesenchymal stem cells, higher levels inhibit their differentiation into adipocytes. **Cell Death Dis 4:**e594, 2013

Sabatti C, Service S, Freimer N: False discovery rate in linkage and association genome screens for complex disorders. **Genetics 164:**829-833, 2003

Schena M, Shalon D, Davis RW, Brown PO: Quantitative monitoring of gene expression patterns with a complementary DNA microarray. **Science 270:**467-470, 1995

Scott MA, Nguyen VT, Levi B, James AW: Current methods of adipogenic differentiation of mesenchymal stem cells. **Stem Cells Dev 20:**1793-1804, 2011

Segales J, Perdiguero E, Munoz-Canoves P: Regulation of Muscle Stem Cell Functions: A Focus on the p38 MAPK Signaling Pathway. **Front Cell Dev Biol 4:**91, 2016

Shen J, James AW, Zhang X, Pang S, Zara JN, Asatrian G, et al: Novel Wnt Regulator NEL-Like Molecule-1 Antagonizes Adipogenesis and Augments Osteogenesis Induced by Bone Morphogenetic Protein 2. **Am J Pathol 186:**419-434, 2016

Singh K, Nandyala SV, Marquez-Lara A, Fineberg SJ: Epidemiological trends in the utilization of bone morphogenetic protein in spinal fusions from 2002 to 2011. **Spine (Phila Pa 1976) 39:**491-496, 2014

Somoza RA, Welter JF, Correa D, Caplan AI: Chondrogenic differentiation of

mesenchymal stem cells: challenges and unfulfilled expectations. **Tissue Eng Part B Rev 20:**596-608, 2014

Stenderup K, Justesen J, Clausen C, Kassem M: Aging is associated with decreased maximal life span and accelerated senescence of bone marrow stromal cells. **Bone 33:**919-926, 2003

Stenderup K, Justesen J, Eriksen EF, Rattan SI, Kassem M: Number and proliferative capacity of osteogenic stem cells are maintained during aging and in patients with osteoporosis. **J Bone Miner Res 16:**1120-1129, 2001

Stolzing A, Coleman N, Scutt A: Glucose-induced replicative senescence in mesenchymal stem cells. **Rejuvenation Res 9:**31-35, 2006

Talavera-Adame D, Gupta A, Kurtovic S, Chaiboonma KL, Arumugaswami V, Dafoe DC: Bone morphogenetic protein-2/-4 upregulation promoted by endothelial cells in coculture enhances mouse embryoid body differentiation. **Stem Cells Dev 22:**3252-3260, 2013

Vaes BL, Dechering KJ, Feijen A, Hendriks JM, Lefevre C, Mummery CL, et al: Comprehensive microarray analysis of bone morphogenetic protein 2-induced osteoblast differentiation resulting in the identification of novel markers for bone development. **J Bone Miner Res 17:**2106-2118, 2002

Vishnubalaji R, Al-Nbaheen M, Kadalmani B, Aldahmash A, Ramesh T: Comparative investigation of the differentiation capability of bone-marrow- and adipose-derived mesenchymal stem cells by qualitative and quantitative analysis. **Cell Tissue Res 347:**419-427, 2012

Wagner W, Horn P, Castoldi M, Diehlmann A, Bork S, Saffrich R, et al: Replicative Senescence of Mesenchymal Stem Cells: A Continuous and

Organized Process, in **PLoS ONE**, 2008, Vol 3, pp e2213-2212

Wang EA, Israel DI, Kelly S, Luxenberg DP: Bone morphogenetic protein-2 causes commitment and differentiation in C3H10T1/2 and 3T3 cells. **Growth Factors 9:**57-71, 1993

Wang L, Li L, Ran X, Long M, Zhang M, Tao Y, et al: Lipopolysaccharides reduce adipogenesis in 3T3-L1 adipocytes through activation of NF-kappaB pathway and downregulation of AMPK expression. **Cardiovasc Toxicol 13:**338-346, 2013

Wilde JM, Gumucio JP, Grekin JA, Sarver DC, Noah AC, Ruehlmann DG, et al: Inhibition of p38 mitogen-activated protein kinase signaling reduces fibrosis and lipid accumulation after rotator cuff repair. **J Shoulder Elbow Surg 25:**1501-1508, 2016

Wu L, Cai X, Dong H, Jing W, Huang Y, Yang X, et al: Serum regulates adipogenesis of mesenchymal stem cells via MEK/ERK-dependent PPARgamma expression and phosphorylation. **J Cell Mol Med 14:**922-932, 2010

Xu C, Wang J, Zhu T, Shen Y, Tang X, Fang L, et al: Cross-Talking Between PPAR and WNT Signaling and its Regulation in Mesenchymal Stem Cell Differentiation. **Curr Stem Cell Res Ther 11:**247-254, 2016

Yoon BH, Esquivies L, Ahn C, Gray PC, Ye SK, Kwiatkowski W, et al: An activin A/BMP2 chimera, AB204, displays bone-healing properties superior to those of BMP2. **J Bone Miner Res 29:**1950-1959, 2014

Yu WH, Li FG, Chen XY, Li JT, Wu YH, Huang LH, et al: PPARgamma suppression inhibits adipogenesis but does not promote osteogenesis of

human mesenchymal stem cells. **Int J Biochem Cell Biol 44:**377-384, 2012

Yuan Z, Li Q, Luo S, Liu Z, Luo D, Zhang B, et al: PPARgamma and Wnt Signaling in Adipogenic and Osteogenic Differentiation of Mesenchymal Stem Cells. **Curr Stem Cell Res Ther 11:**216-225, 2016

Yue B, Lu B, Dai KR, Zhang XL, Yu CF, Lou JR, et al: BMP2 gene therapy on the repair of bone defects of aged rats. **Calcif Tissue Int 77:**395-403, 2005

Zhang D, Lu H, Chen Z, Wang Y, Lin J, Xu S, et al: High glucose induces the aging of mesenchymal stem cells via Akt/mTOR signaling. **Mol Med Report 16:**1685-1690, 2017.

Zhang H, Lu W, Zhao Y, Rong P, Cao R, Gu W, et al: Adipocytes derived from human bone marrow mesenchymal stem cells exert inhibitory effects on osteoblastogenesis. **Curr Mol Med 11:**489-502, 2011

Zhang S, Fei T, Zhang L, Zhang R, Chen F, Ning Y, et al: Smad7 antagonizes transforming growth factor beta signaling in the nucleus by interfering with functional Smad-DNA complex formation. **Mol Cell Biol 27:**4488-4499, 2007

Zhang Y, Shao J, Wang Z, Yang T, Liu S, Liu Y, et al: Growth differentiation factor 11 is a protective factor for osteoblastogenesis by targeting PPARgamma. **Gene 557:**209-214, 2015

Zheng GB, Yoon BH, Lee JH: Comparison of the osteogenesis and fusion rates between activin A/BMP-2 chimera (AB204) and rhBMP-2 in a beagle's posterolateral lumbar spine model. **Spine J 17:**1529-1536, 2017

Zhuang H, Zhang X, Zhu C, Tang X, Yu F, Shang GW, et al: Molecular Mechanisms of PPAR-gamma Governing MSC Osteogenic and Adipogenic

Differentiation. **Curr Stem Cell Res Ther 11:**255-264, 2016

국문 초록

목 적: 중배엽 줄기세포 (mesenchymal stem cell)는 조골세포 (osteoblast), 지방세포 (adipocyte), 연골세포 (chondrocyte) 등의 중배엽 기원의 다양한 종류의 세포로 분화할 수 있는 능력을 가진 세포이다. 골형성 단백질-2 (BMP-2)는 조골세포로의 분화를 유도할 수 있는 일련의 연쇄 반응 (cascade)을 유도할 수 있는 강력한 물질이다. 최근, BMP-2 는 고령의 환자에서 척추 유합술시 골유합 대체제로 시도되고 있다. 하지만, BMP-2 및 노화의 영향에 따른 중배엽 줄기세포의 분화에 대해 알려진 바가 별로 없는 것은 BMP-2 를 적극적으로 사용하는데 제한점이 되고 있다. 이런 점에서 재조합 인간 BMP-2 (rhBMP-2)가 중배엽 줄기 세포의 조골세포, 지방세포로의 분화에 미치는 영향을 노화 세포와 젊은 세포 (대조군) 간에 비교하고자 하였다.

대상 및 방법: 세포의 노화는 고농도 당을 포함한 배지에서 반복 배양 (replicative passage)을 함으로써 유도하였다. 노화 중배엽 줄기세포를 확인하기 위해서, Senescence-associated ß-galactosidase (SA-ß-gal) 염색과 관련 표시자 (p16, p21, p53)를 사용하였다. 노화 세포 및 대조군 세포를 각각 다른 농도의 BMP-2 (0, 25, 100, 250, and 500 ng/ml) 를 포함한 골분화 배지 및 지방분화 배지에 배양하였다. 칼슘 분석 시험 및 지방 생성 분석 시험, 특정 염색법 (Alkaline Phosphatase, Alizarin Red S, Oil red O)을 통해서 표현형을 비교하였고, 실시간 중합 효소 연쇄 반응 (real-time PCR), 웨스턴 블롯 분석, 마이크로어레이를 이용하여 노화 세포 및 대조군 세포간 유전자 발현 패턴의 차이를 분석하였다. 마이크로어레이는 4 개의 다른 종류의 세포 (BMP-2 처치 전과 처치 후 노화 세포 및 대조군 세포)를 이용하였고, GSEA (Gene Set Enrichment Analysis), leading edge subset 분석, 메타코어 분석을 하였다.

결 과: 고농도 당 (22 mM) 배지에서 반복 배양하여 유도한 노화 세포는 노화 관련 표지자를 통해 잘 발현되었음이 확인되었다. 노화 중배엽 줄기세포는 대조군 세포에 비해, BMP-2 에 의한 골 분화는 감소하였다. 노화 중배엽 줄기세포에서, ALP 활성도 ($P < 0.001$)와 Ca^{++}유리 ($P = 0.005$)는 상대적으로 낮았으며, BMP-2 용량에 따라 증가되는 반응을 보였다. 또한, Runx2, Bone sialoprotein (BSP),

오스테오칼신 (OCN) mRNA 발현이 노화 세포에서 상대적으로 낮았다. 하지만, 노화 중배엽 줄기세포에서 BMP-2 에 의한 지방 분화는 대조군 세포와 비슷하였다. 지방 생성 분석 시험에 의해 두 군간에 지방 분화 능력이 차이가 없음이 확인되었으며 (P = 0.279), PPARɣ의 발현도 두 군간에 차이가 없었다. 이와 같은 결과는 웨스턴 블롯 검사를 이용하여 단백질 수준에서도 확인되었다.

마이크로어레이 결과, BMP-2 처치한 대조군 세포 및 처치하지 않은 노화 세포에 비해, BMP-2 처치한 노화 세포에서 더 많은 유전자가 상향 조절 (up-regulation)됨을 확인하였다. 노화 및 지방생성 관련 유전자 군은 BMP-2 처치시 대조군 세포에 비해 노화 세포에서 더 상향 조절되었고 의미있게 enrichment 되었다. BMP 관련 leading edge 군에서, 6 개의 군집된 유전자 (CHRDL1, NOG, SMAD1, SMAD7, FST, BAMBI) 가 노화 세포에서 상향 조절되었다. 메타코어 분석에서, BMP-2 에 대한 반응은 대조군 세포에서의 BMP/SMAD 경로에 비해, 노화 세포에서는 NF-kB 나 p38 MAPK 경로가 중요할 것으로 생각되었다.

결 론: 노화 중배엽 줄기세포는 대조군 세포에 비해 BMP-2의 자극에 의해 골분화는 감소하고, 지방 분화는 큰 변화가 없었다. 노화 중배엽 줄기세포에서 BMP-2에 의해 지방세포로의 분화가 상대적으로 우세한 것은 마이크로어레이 분석을 통해서도 확인할 수 있었다. 또한 몇몇 유전자는 중배엽 줄기세포의 분화에 있어서 노화와 연관된

BMP-2의 영향을 결정하는데 관여할 가능성이 있었다. 노화 세포 및 대조군 세포에서 BMP-2에 대한 다른 반응에는 서로 다른 신호 전달 경로가 관여할 것으로 생각된다. 본 연구와 더불어 추가적인 생체내 실험을 통해 BMP-2에 의한 중배엽 줄기세포의 조골세포 및 지방세포로의 분화를 결정하는 신호 전달 경로를 밝힘으로써 임상 영역에서의 BMP-2 사용에 도움을 줄 것으로 생각한다.

색인 단어: 중배엽 줄기 세포 (mesenchymal stem cell); 골 형성 단백질; BMP-2; 분화; 노화; 조골세포; 지방세포; 마이크로어레이

학 번: 2012-31133